

Supporting information

RhNPs supported in N-functionalized mesoporous silica: effect on catalyst stabilization and catalytic activity

^a*Israel T. Pulido-Díaz, ^aAlejandro Serrano-Maldonado, Carlos Cesar López-Suárez, ^aPedro A. Méndez-Ocampo, ^bBenjamín Portales-Martínez, ^cAída Gutiérrez-Alejandre, ^aKarla P. Salas-Martin and Itzel Guerrero-Ríos^{a*}*

^a*Depto. de Química Inorgánica y Nuclear, Facultad de Química, Universidad Nacional Autónoma de México. Av. Universidad 3000, 04510 CDMX, México*

^b*CONACYT, Centro de Investigación en Ciencia Aplicada y Tecnología Avanzada, Laboratorio Nacional de Conversión y Almacenamiento de Energía, Instituto Politécnico Nacional, Calzada Legaría 694, Col. Irrigación, Ciudad de México, 11500, Mexico*

^c*Depto de Ingeniería Química, Facultad de Química, Universidad Nacional Autónoma de México. Av. Universidad 3000, 04510 CDMX, México*

*Corresponding author, E-mail: itzelgr@unam.mx; Tel: +52 55 56223770

1. NMR spectra of $(EtO)_3Si-(CH_2)_3-NAM$

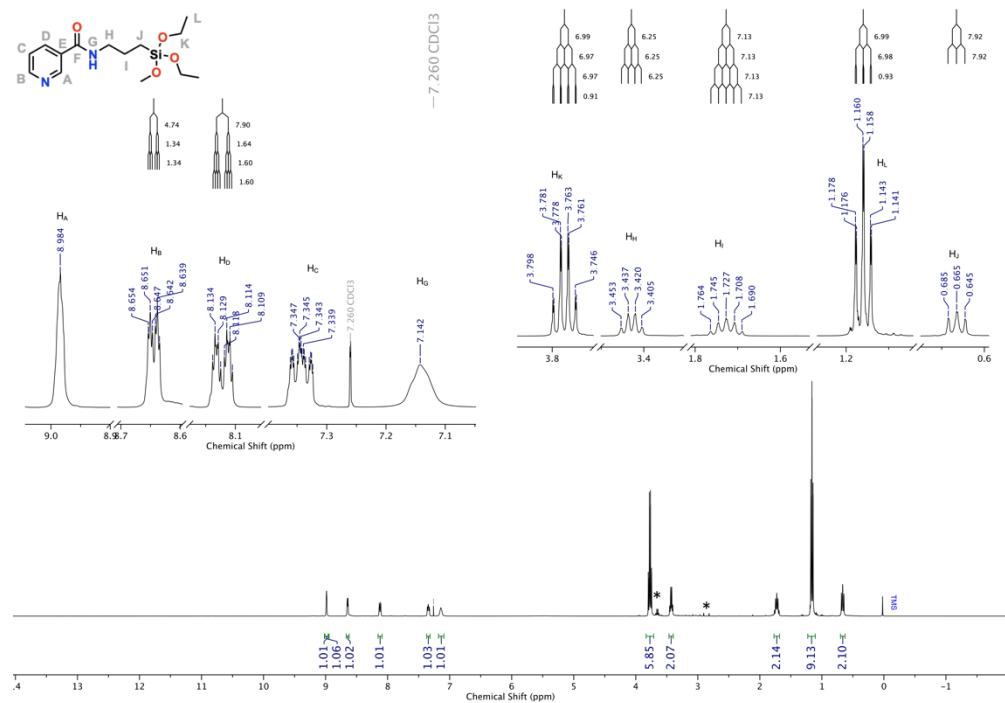


Figure S1 1H -NMR spectra (400.13 MHz, r. t., $CDCl_3$) of N-(3-(triethoxysilyl)propyl) nicotinamide (**NAM**) (*) denotes residual triethylamine on sample.

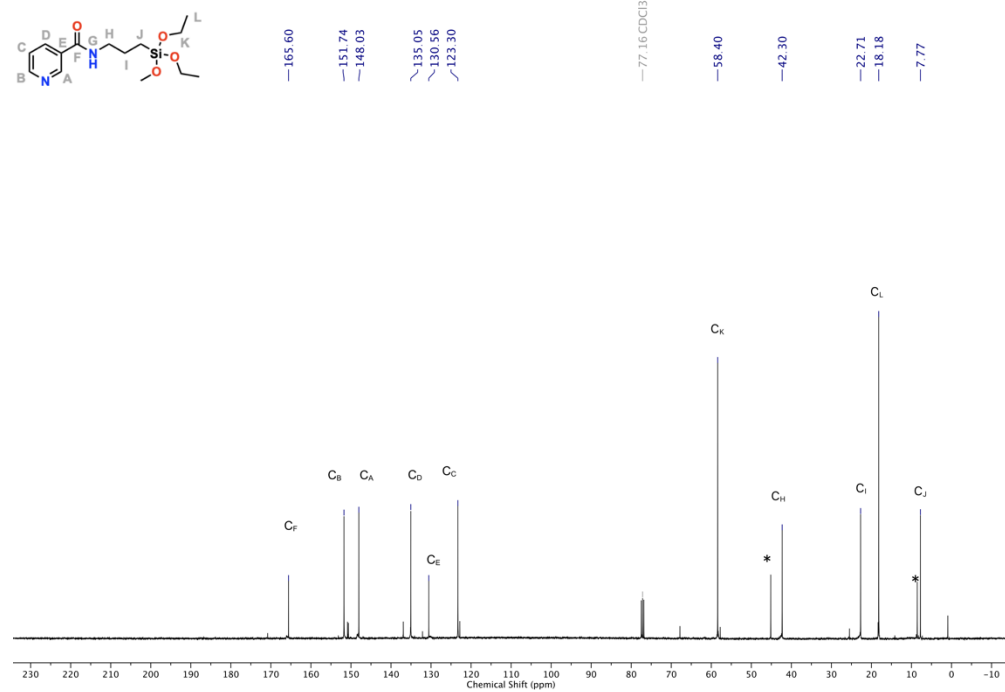


Figure S2 $^{13}C\{^1H\}$ -NMR spectra (100.61 MHz, r. t., $CDCl_3$) of **NAM**. Asterisks (*) denotes residual triethylamine on sample.

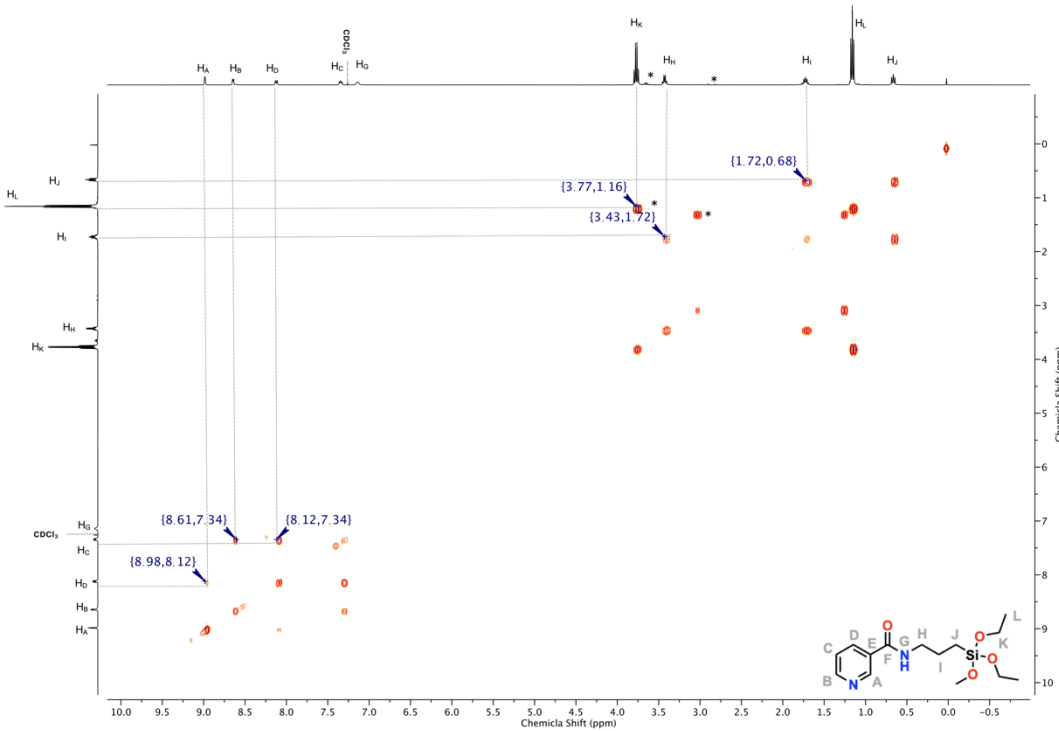


Figure S3 $\{^1\text{H}\}$ COSY-NMR spectra (400.13 MHz, r. t., CDCl_3) of **NAM**. Asterisks (*) denotes residual triethylamine on sample.

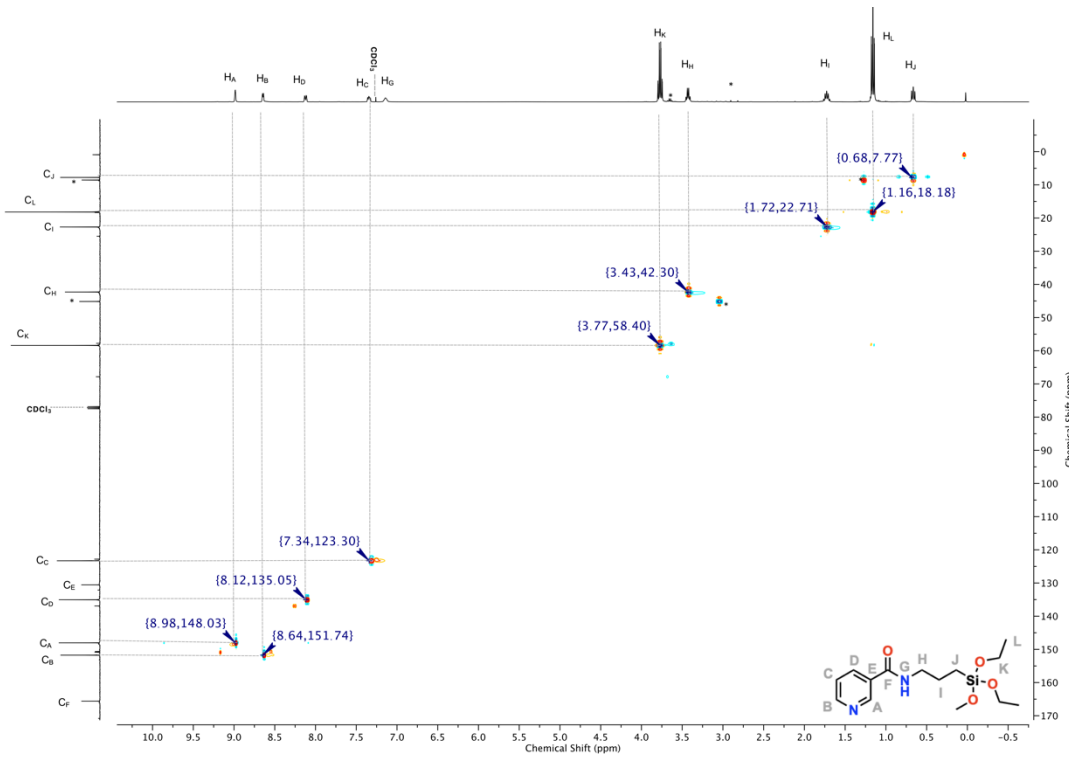


Figure S4 $\{^1\text{H}-^{13}\text{C}\}$ HSQC-NMR spectra (400.13 MHz, r. t., CDCl_3) of **NAM**. Asterisks (*) denotes residual triethylamine on sample

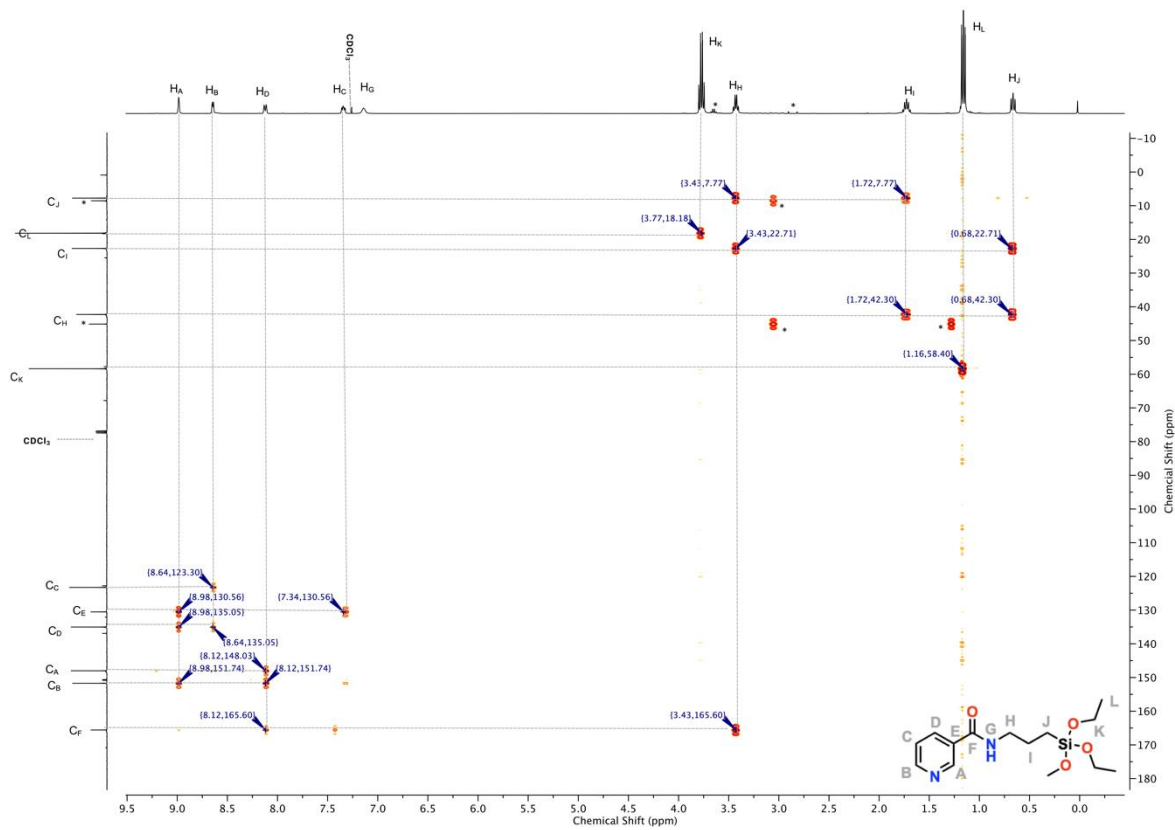


Figure S5 $\{{}^1\text{H}-{}^{13}\text{C}\}$ HMBC-NMR spectra (400.13 MHz, r. t., CDCl_3) of **NAM**. Asterisks (*) denotes residual triethylamine on sample.

2. FT-IR spectra of supported RhNPs.

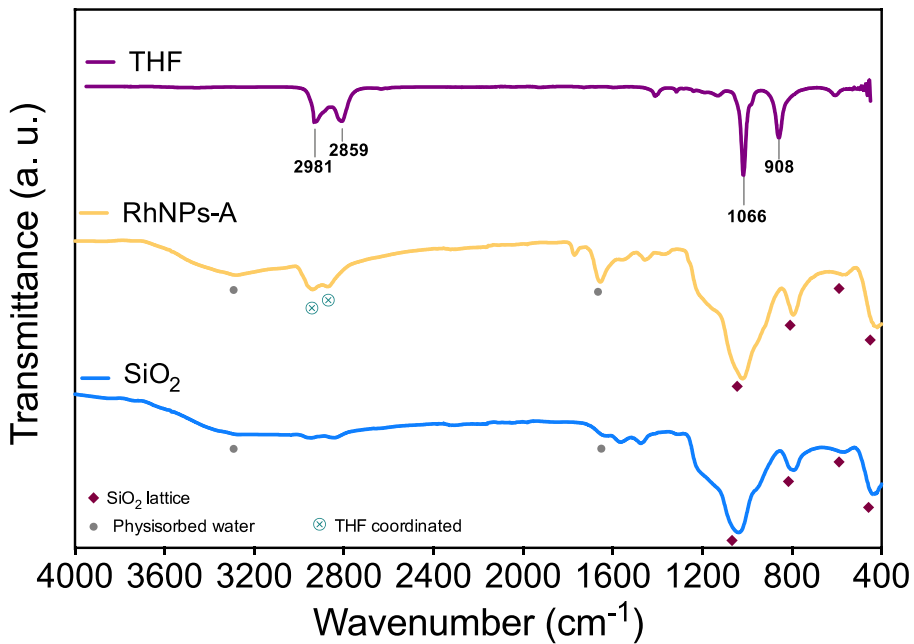


Figure S6- IR spectra of SiO₂, RhNPs-A and THF.

Table S1 Characteristic absorption bands ν (cm⁻¹) in IR spectra of N-grafted silicas and supported RhNPs.

Assignment	SiO ₂	RhNPs-A	SiO ₂ -APTES	RhNPs-B	SiO ₂ -NAM	RhNPs-C
ν (Si-O-H) and ν (HO-H) _{Phys.}	3275br 1642w	3277br 1655w	3295br 1635w	3273br 1652m	3298br ----	3296br ---
ν (Si-O-Si)	1039s 947sh 788m	1012s 932sh 791m	1047s 965sh 795m	1043s 961sh 793m	1046s 959sh 795m	1051s 957sh 809m
δ (Si-O)	430m	410m	443m	431m	433m	445m
ν (C-H)	---	---	2923m 2853m	2924m 2854m	2919m 2841m	2926m 2861m
ν (C-N) _{amine}	---	---	1219sh	1215sh	---	---
ν (N-H)	---	---	1477w	1465w	1475m	1463m
δ (N-H)	---	---	1555w	1561w	1546m	1541m
γ (N-H) _{wagg}	---	---	698vw	---	703vw	699vw
ν (C=O)	---	---	---	---	1640s	1648s
ν_{py} (C=C)	---	---	---	---	1193m	1209m
ν_{py} (C-H)	---	---	---	---	3078w	3091w
ν_{py} (C=N)	---	---	---	---	1427m	1417m

s (strong), br (broad), m (medium), w (weak), vw (very weak), sh (shoulder), py (pyridine)

3. XPS analysis of RhNPs

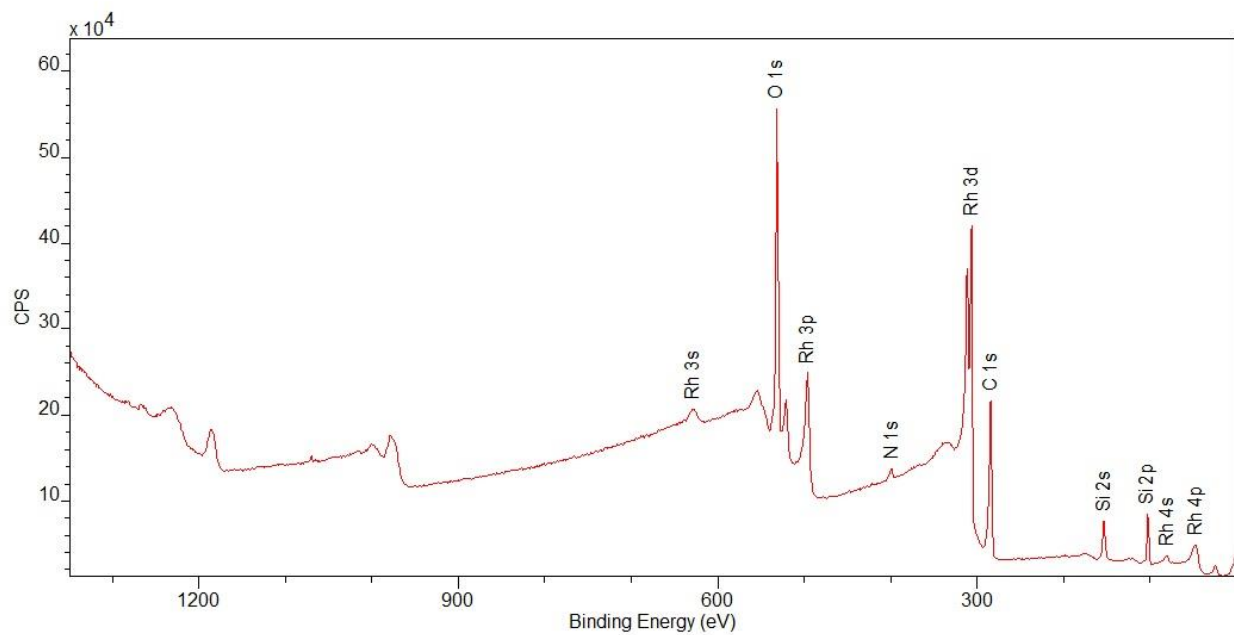


Figure S7 XPS survey of RhNPs-B.

Table S2 Element distribution on surface of RhNPs-B by XPS.

Element	Atomic %	Weight %
C 1s	40.3	19.8
N 1s	1.5	0.8
O 1s	36.7	24.1
Si 2p	11.5	13.2
Rh 3d	10.0	42.1

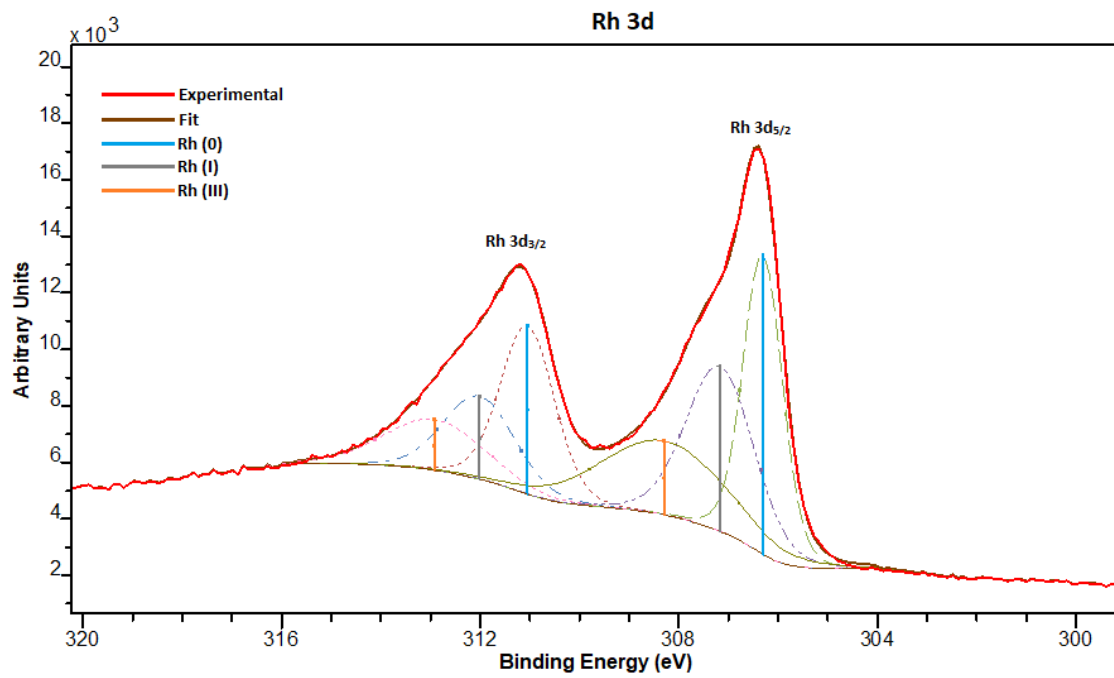


Figure S8 High resolution-XPS Rh 3d of RhNPs-B.

Table S3 Rhodium species distribution on surface of **RhNPs-B** by XPS.

Rh 3d (BE, eV)			Area % (3d _{5/2})
	3/2	5/2	
Rh (0)	311.05	306.31	36.4
Rh (I)	312.01	307.17	34.7
Rh (III)	312.93	308.29	28.9

Residual STD = 1.07199

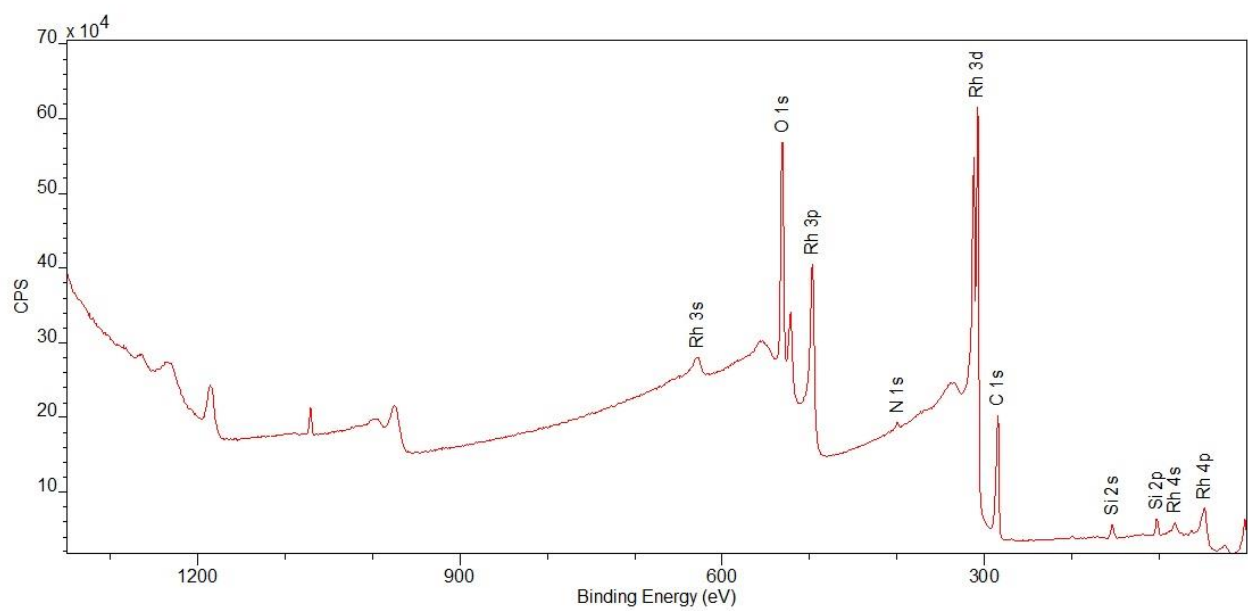


Figure S9 XPS survey of RhNPs-C.

Table S4 Element distribution on surface of RhNPs-C by XPS.

Element	Atomic %	Weight %
C 1s	39.0	16.1
N 1s	0.9	0.5
O 1s	40.6	22.5
Si 2p	5.6	5.1
Rh 3d	13.9	55.8

4. Thermal decomposition data of synthesized materials

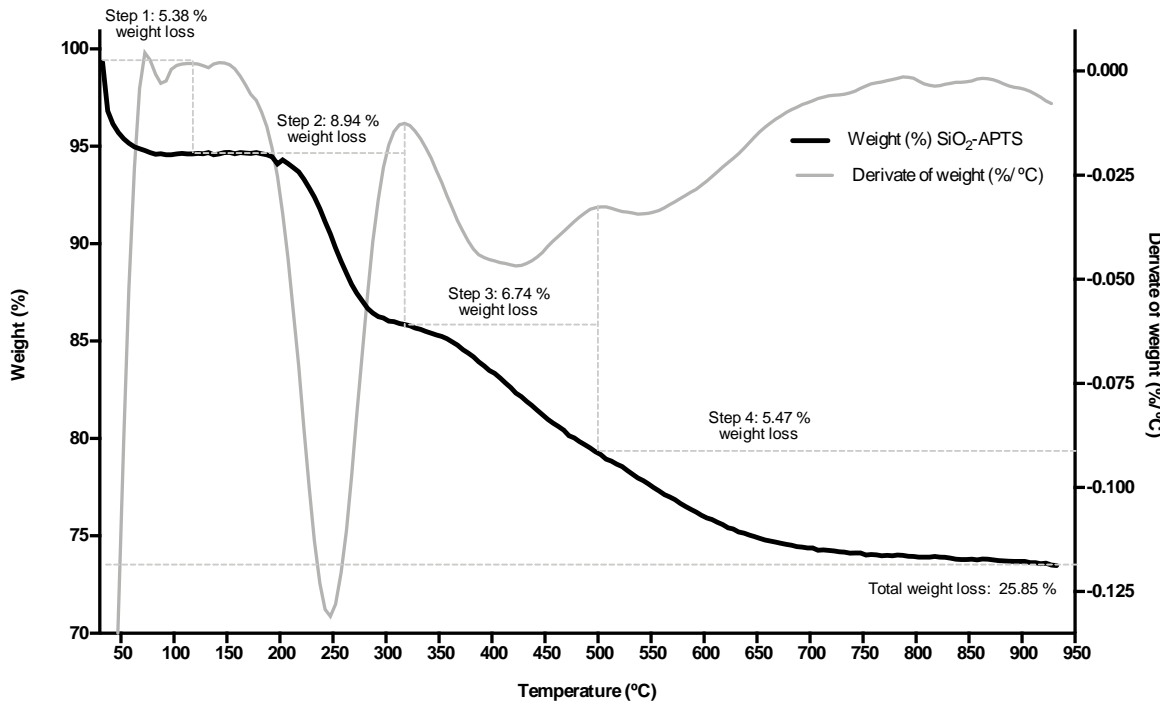


Figure S10 Thermal decomposition data of **SiO₂-APTES** run in air at heating rate of 1 °C/min.

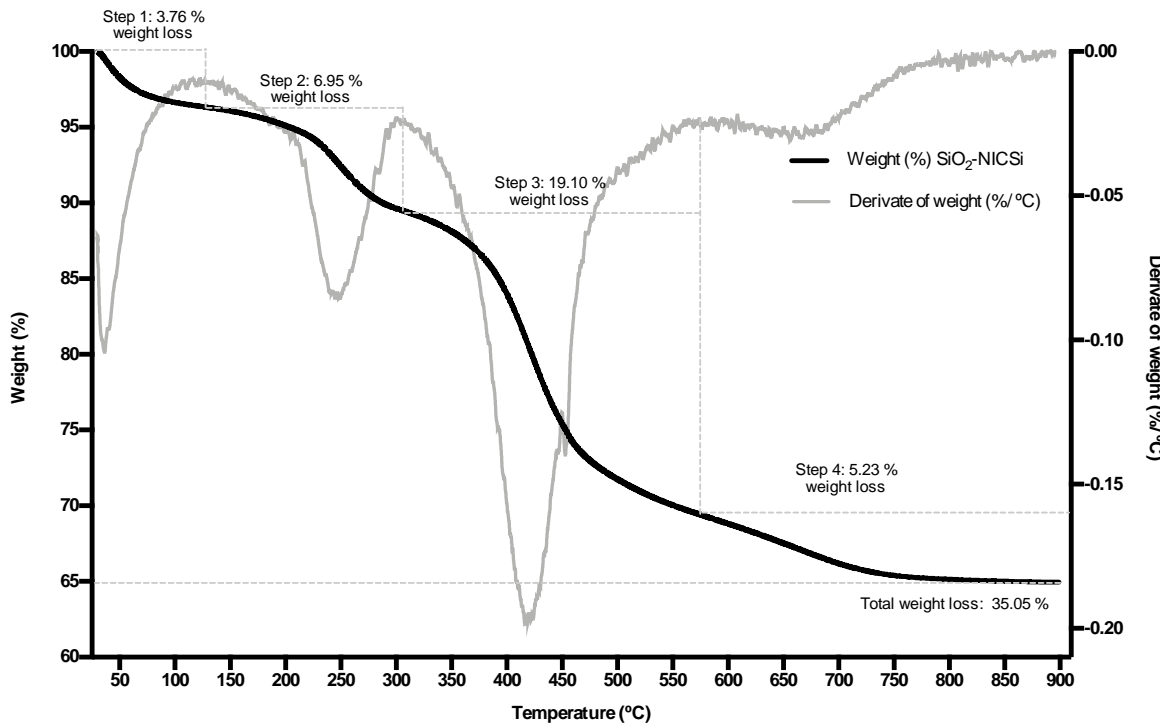


Figure S11 Thermal decomposition data of **SiO₂-(CH₂)₃-NAM** run in air at heating rate of 5 °C/min.

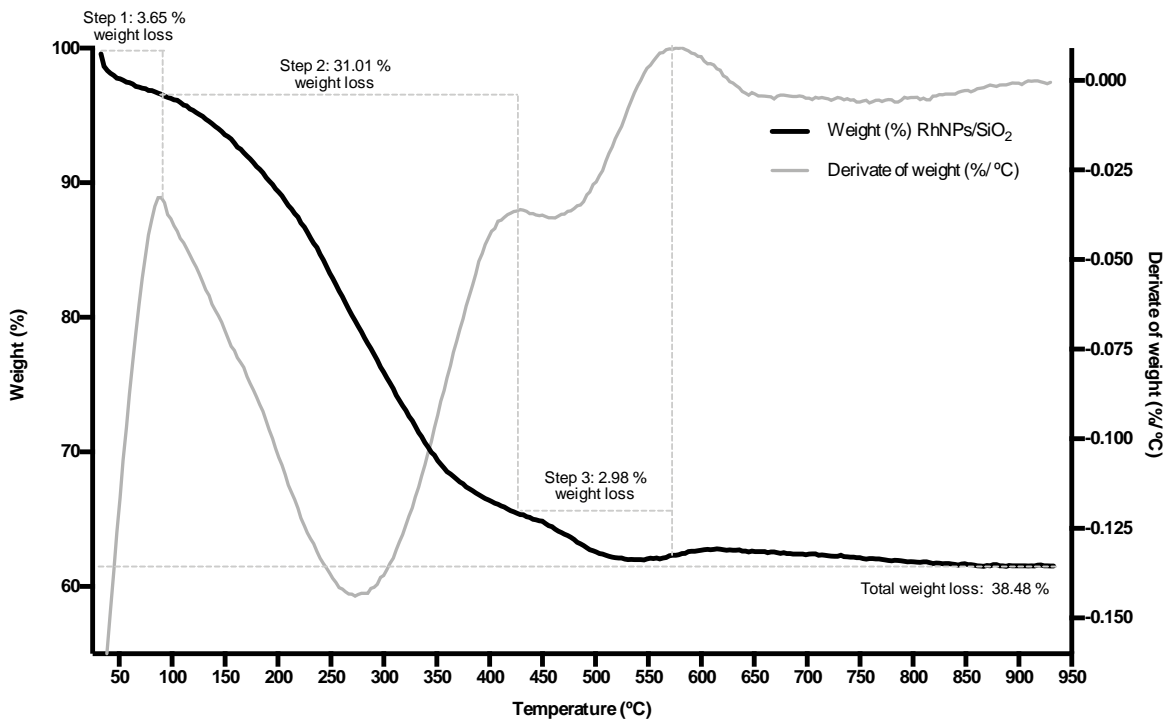


Figure S12 Thermal decomposition data of RhNPs-A run in air at a heating rate of 1 °C/min.

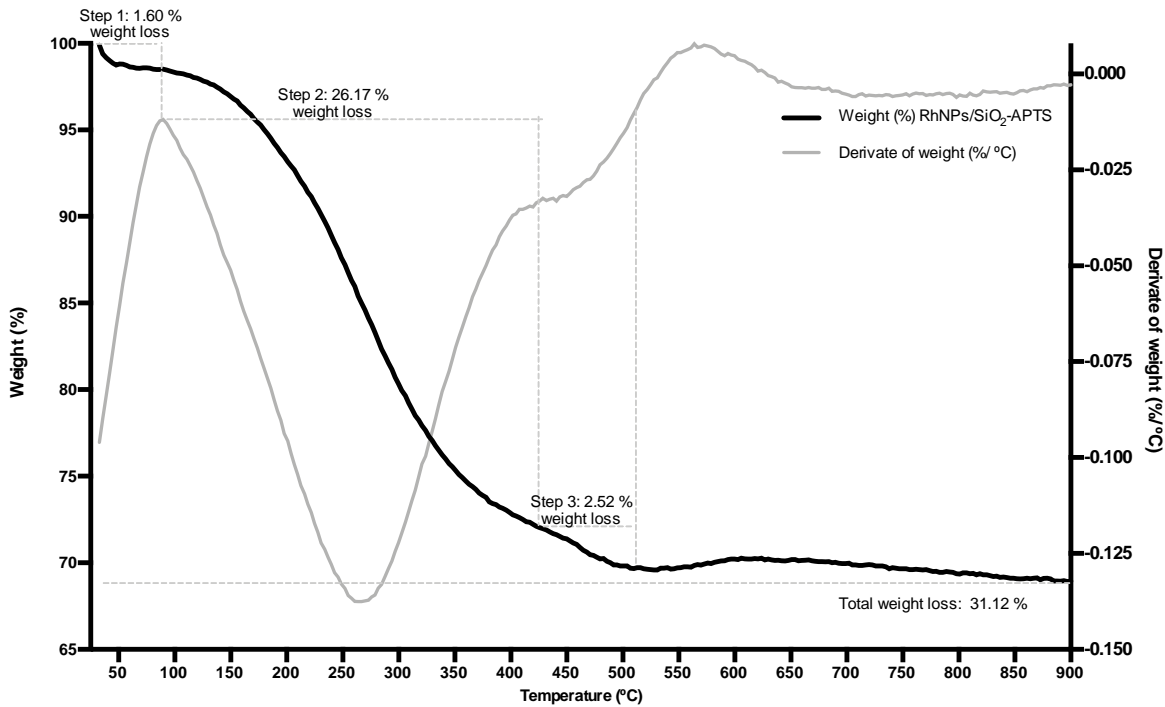


Figure S13 Thermal decomposition data of RhNPs-B run in air at a heating rate of 1 °C/min.

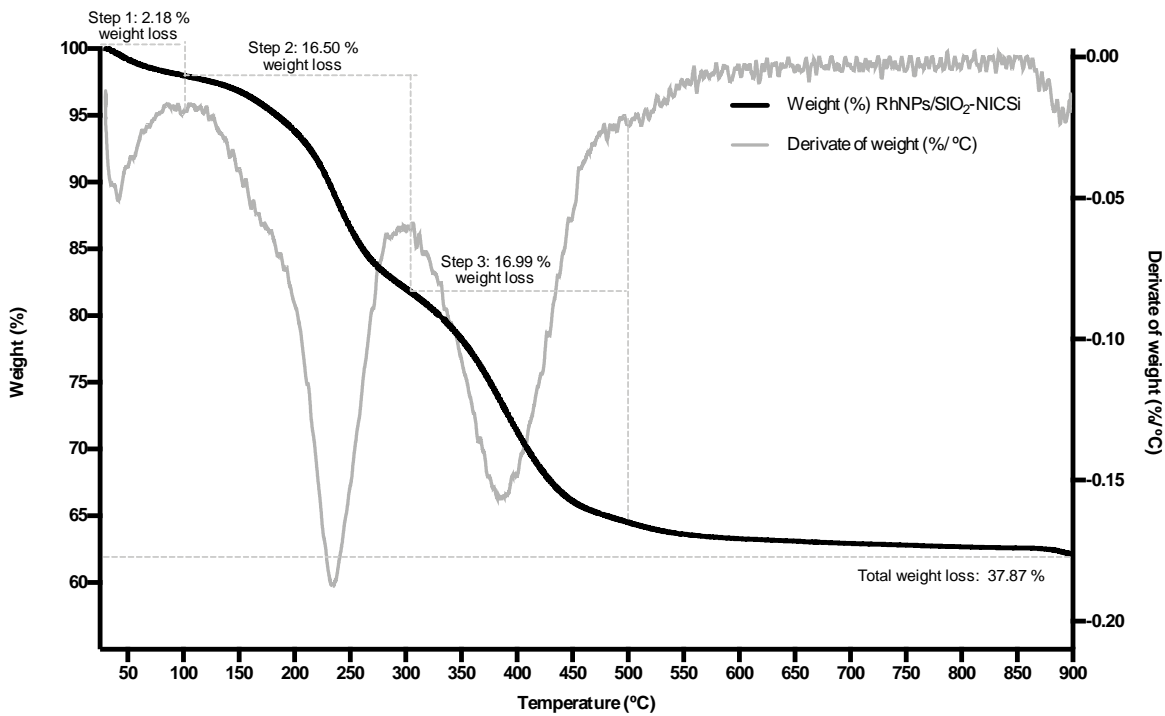


Figure S14 Thermal decomposition data of **RhNPs-C** run in air at heating rate of 5 °C/min.

5. SEM images and particle distribution.

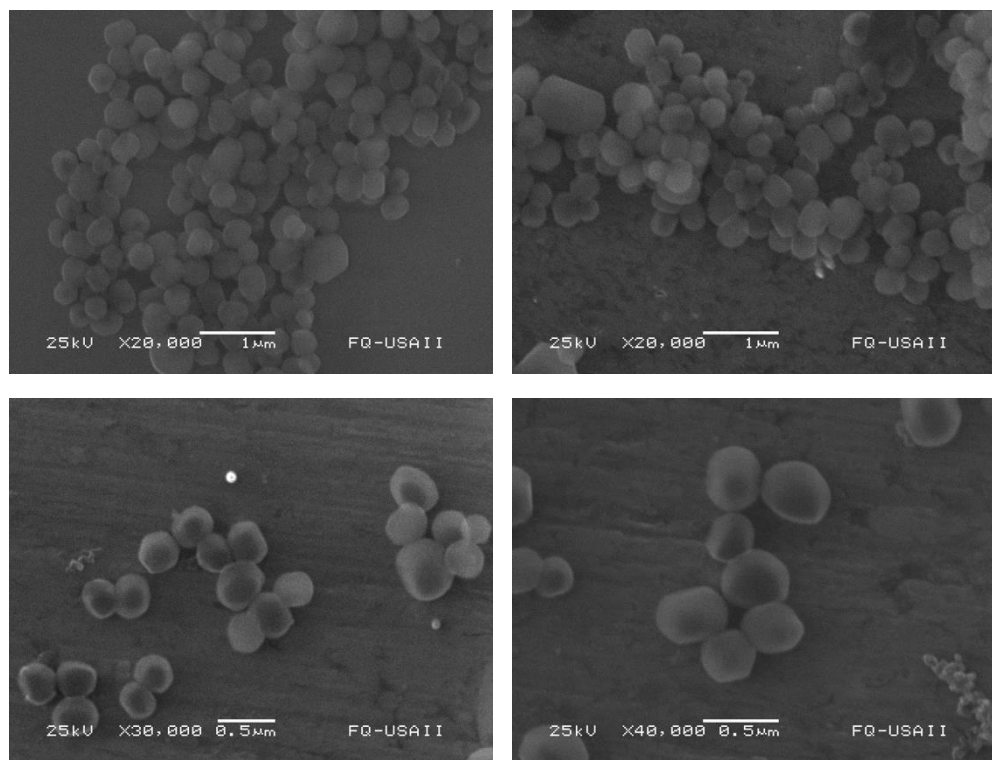


Figure S15 SEM images of functionalized silica **SiO₂-APTES**.

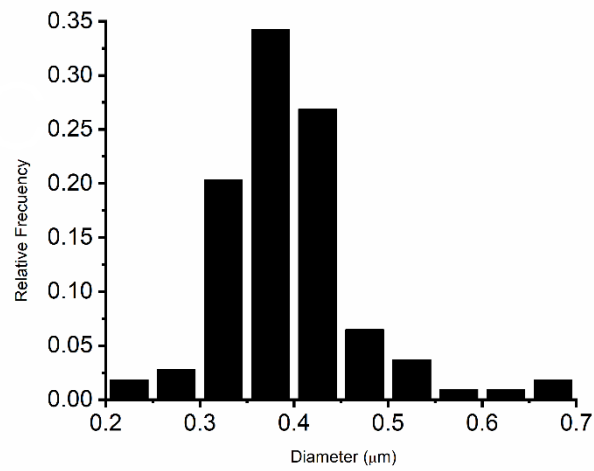


Figure S16 Histogram of the **SiO₂-APTES** particle size distribution. Mean diameter = 393±74 nm (for 108 particles)

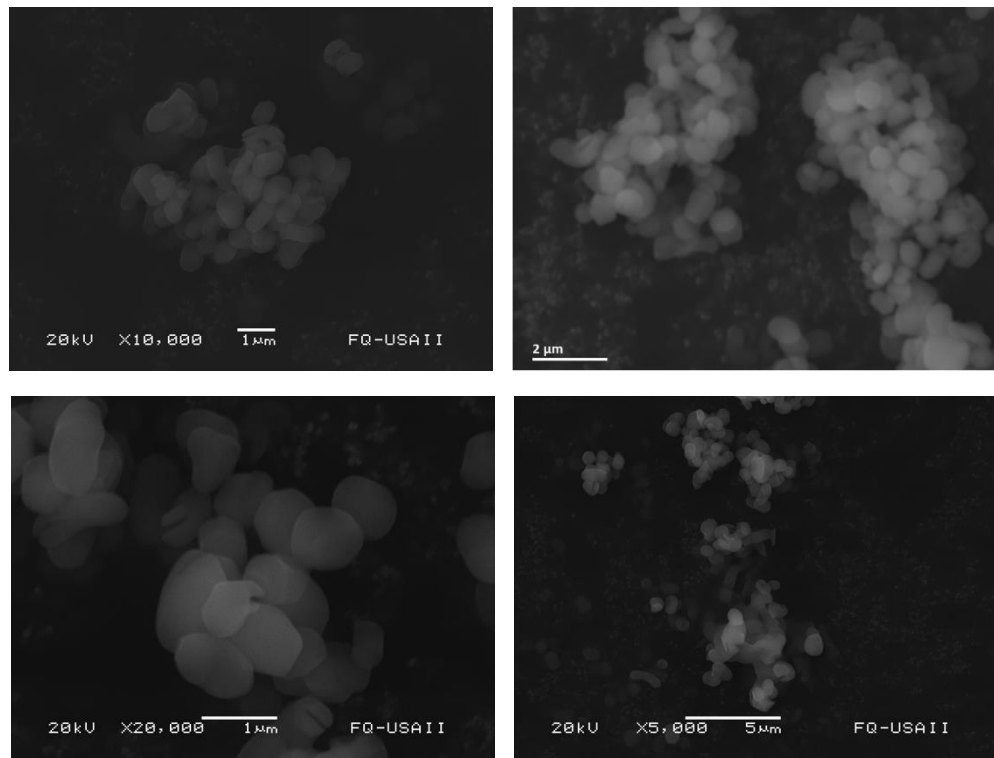


Figure S17 SEM images of functionalized silica $\text{SiO}_2\text{-}(\text{CH}_2)_3\text{-NAM}$.

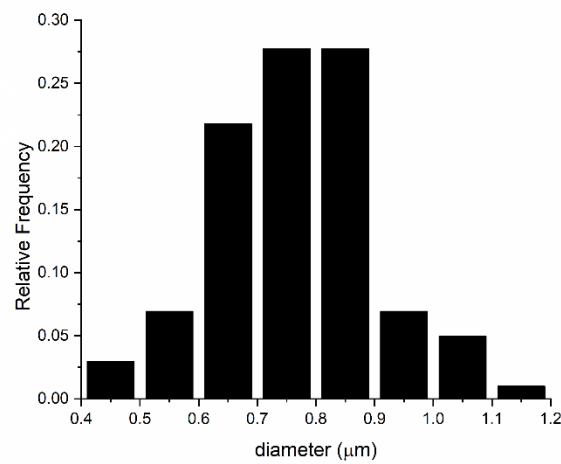


Figure S18 Histogram of the $\text{SiO}_2\text{-}(\text{CH}_2)_3\text{-NAM}$ particle size distribution. Mean diameter = 767 ± 137 nm (for 101 particles)

6. TEM images and EDX analysis

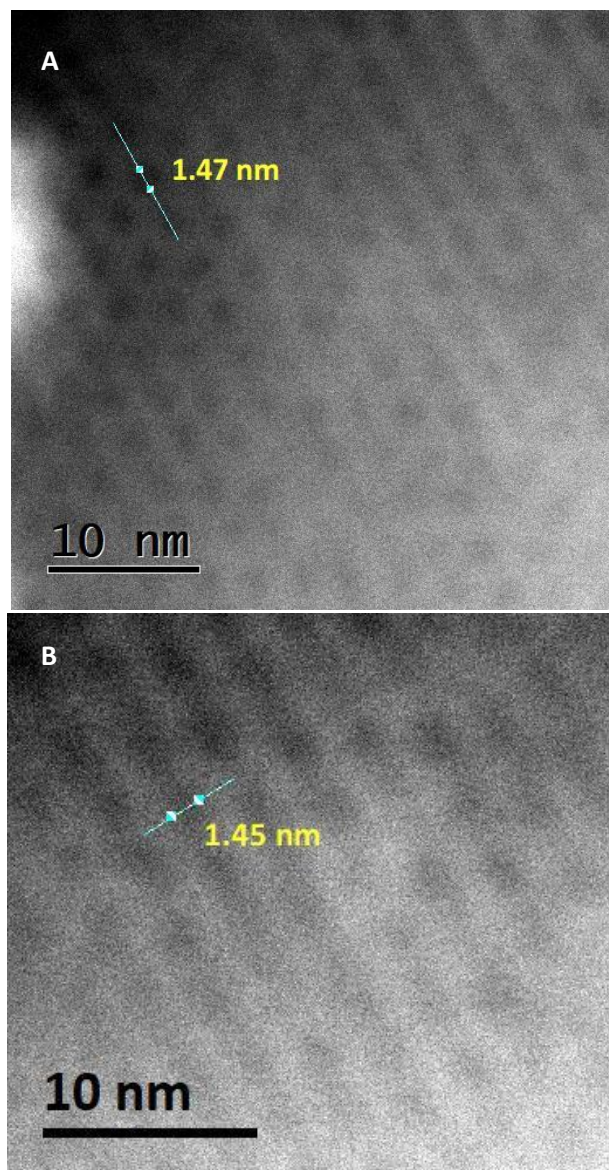


Figure S19 HAADF-STEM images of pristine SiO_2 and FFT of A-B (Pore size measured determined by FFT = 1.4 nm).

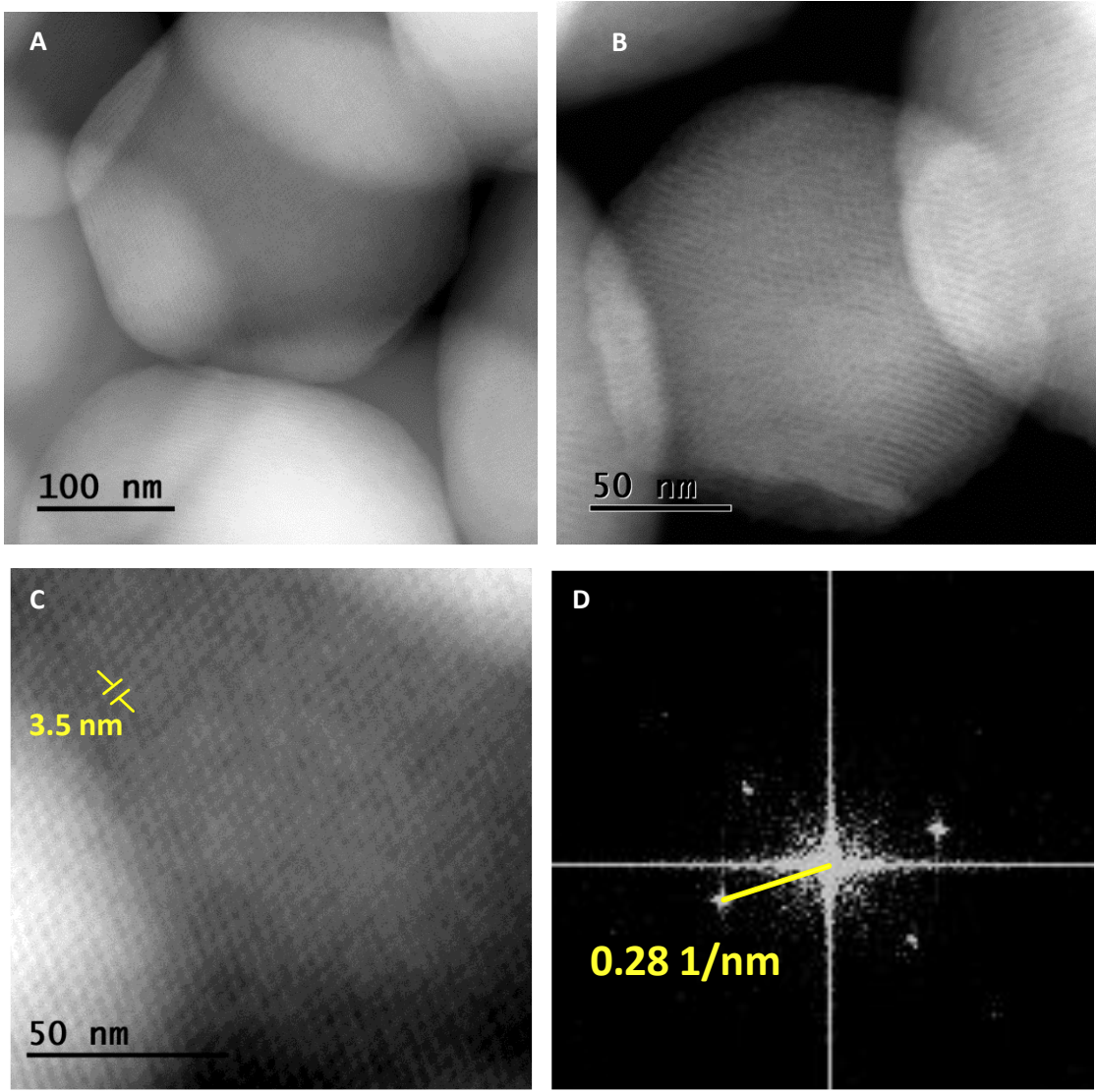


Figure S20 HAADF-STEM images of SiO_2 -APTES (A-C) and FFT of C. (Pore size measured determined by FFT = 3.5 nm).

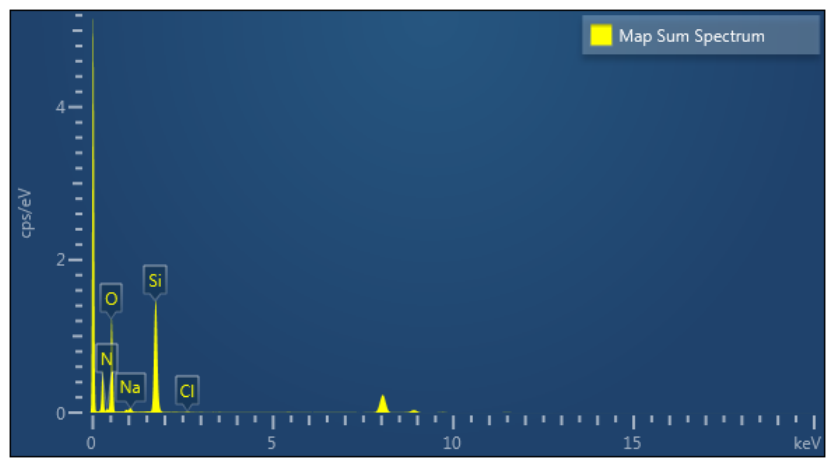


Figure S21 EDX element quantification of SiO_2 -APTES.

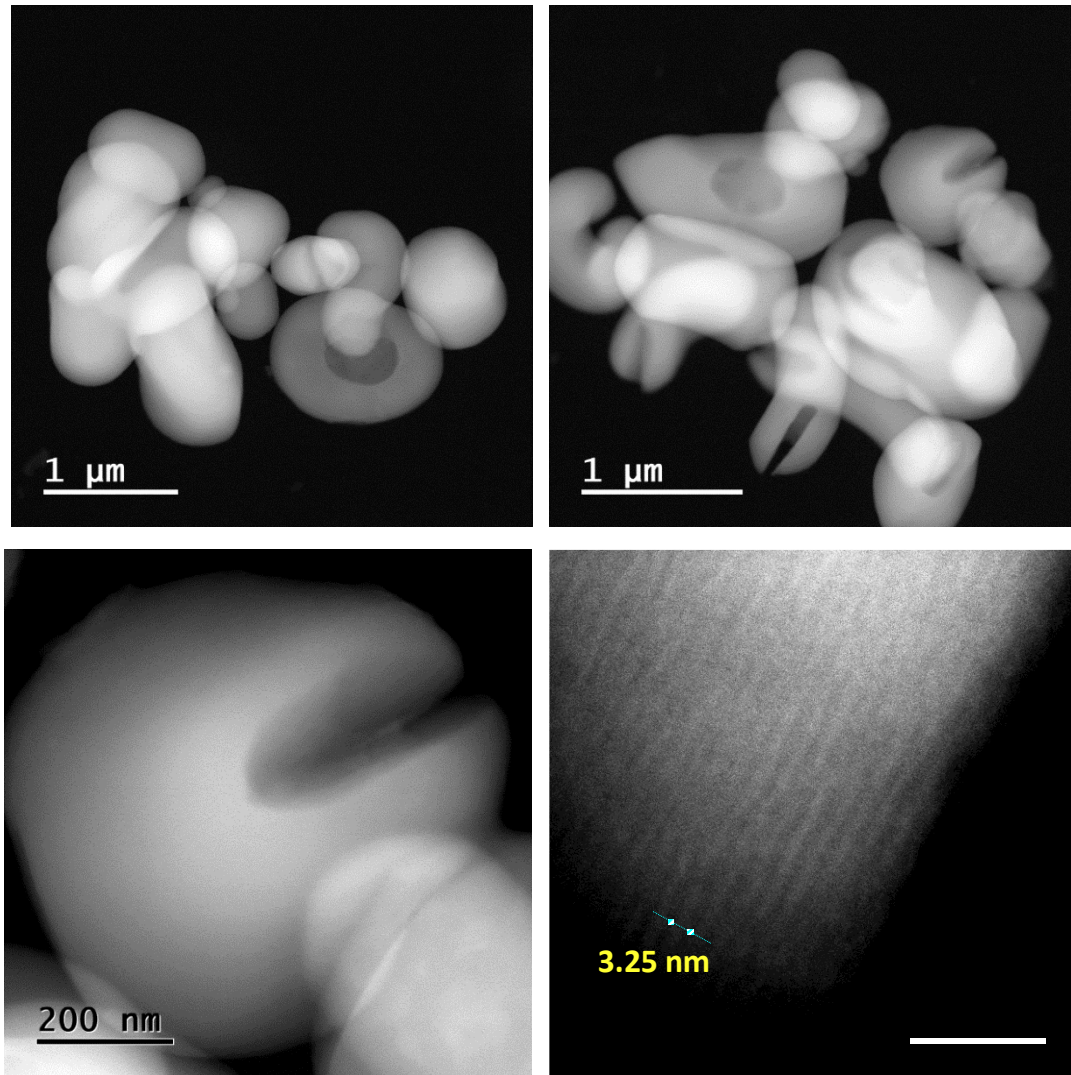


Figure S22 HAADF-STEM images of $\text{SiO}_2\text{-}(\text{CH}_2)_3\text{-NAM}$. (Pore size determined by HAADF-STEM = 3.3 nm)

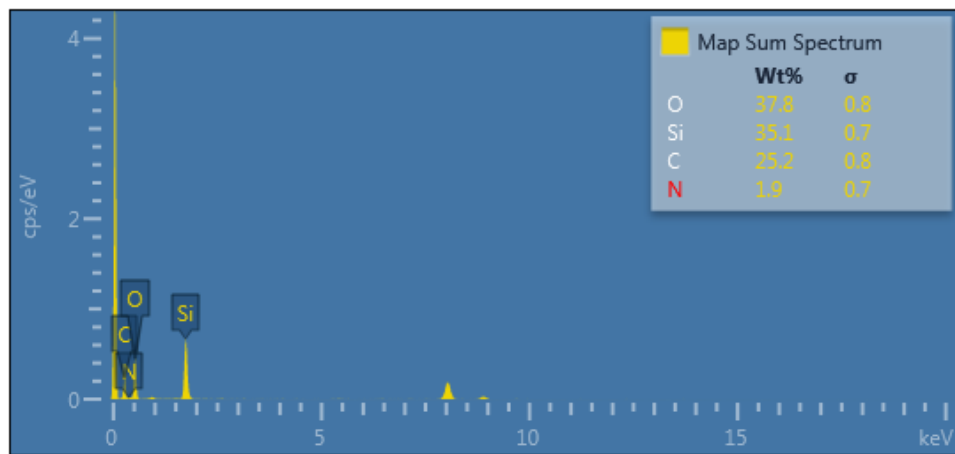


Figure S23 EDX element quantification of $\text{SiO}_2\text{-}(\text{CH}_2)_3\text{-NAM}$.

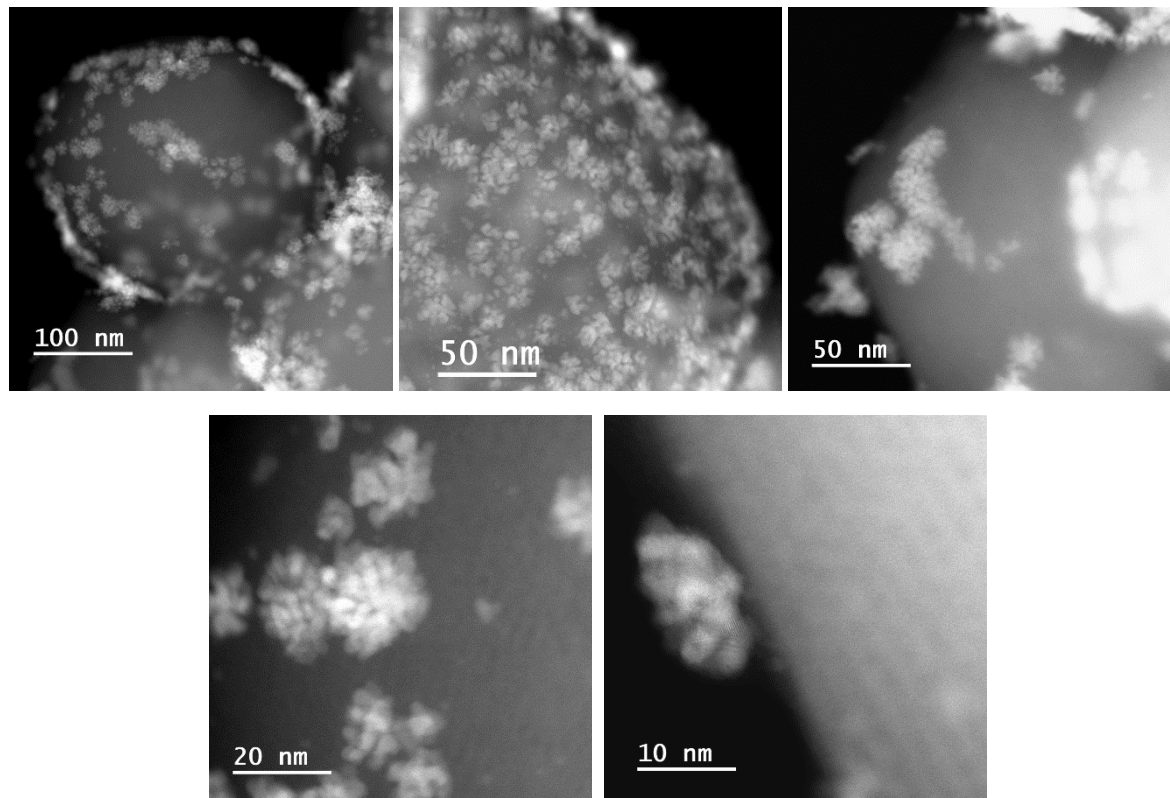


Figure S24 HAADF-STEM images of **RhNPs-A**. (no functionalization)

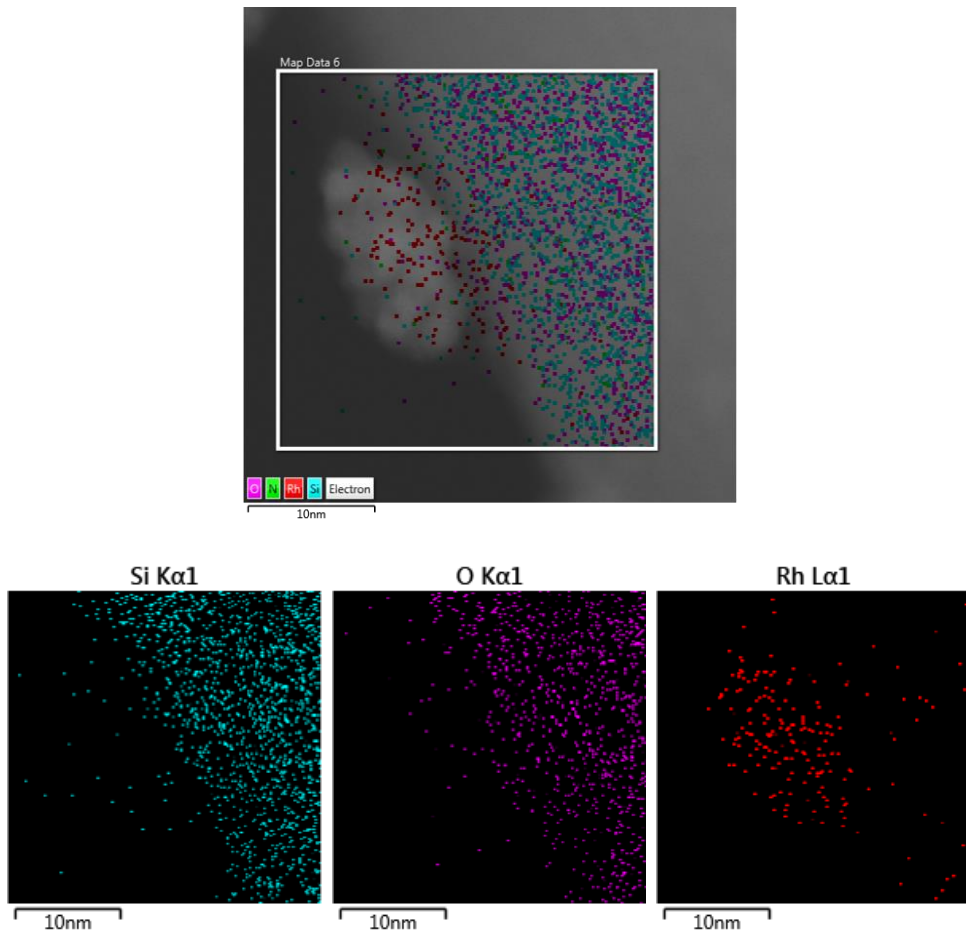


Figure S25 EDX element mapping images of **RhNPs-A.**(no functionalization)

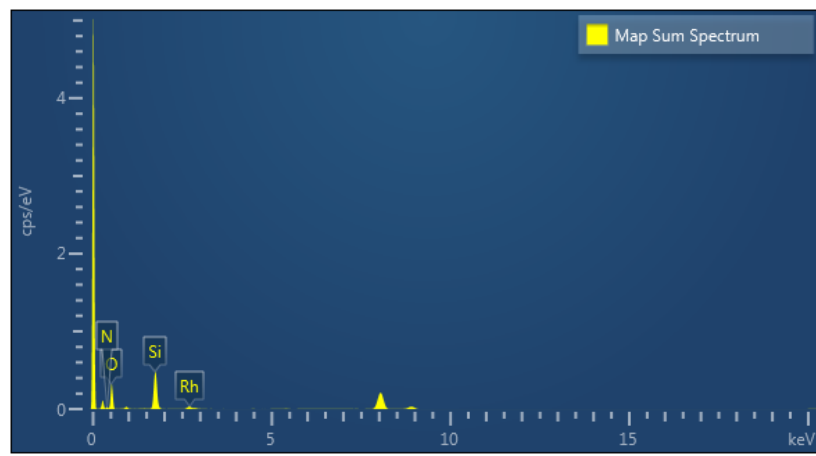


Figure S26 EDX element quantification of **RhNPs-A.** (no functionalization)

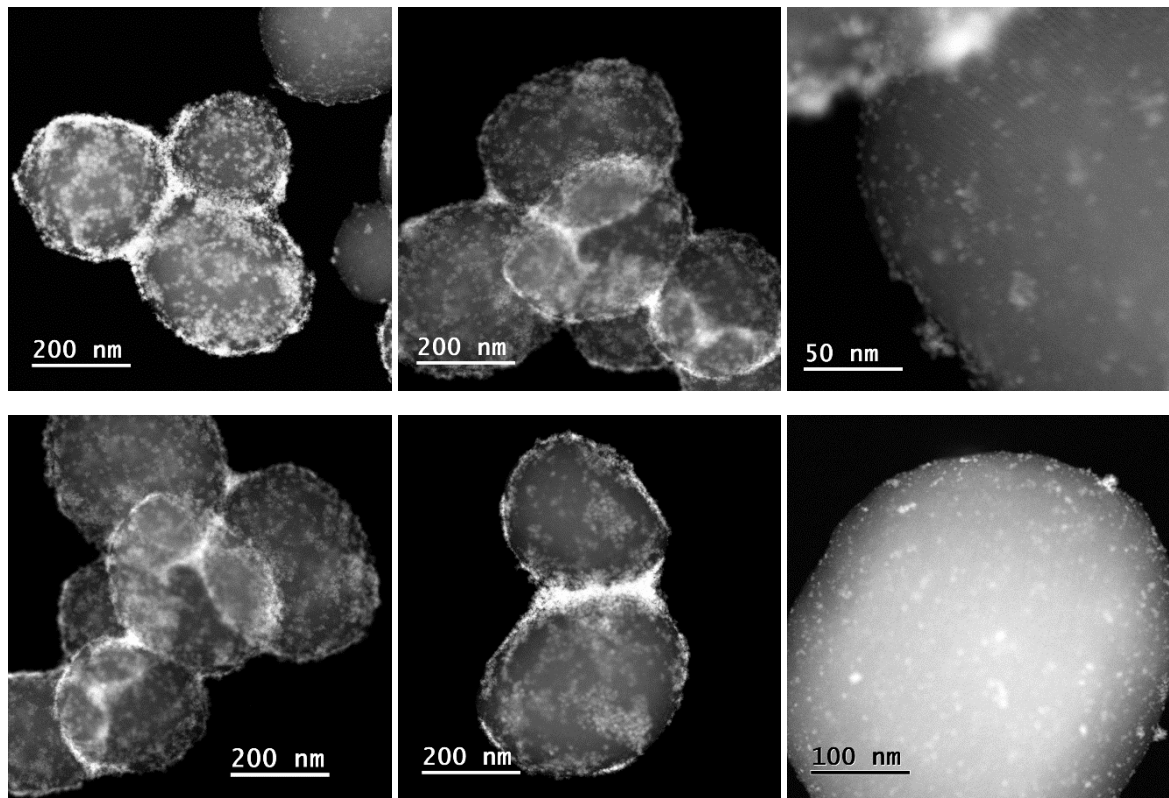


Figure S27 HAADF-STEM images of **RhNPs-B**.

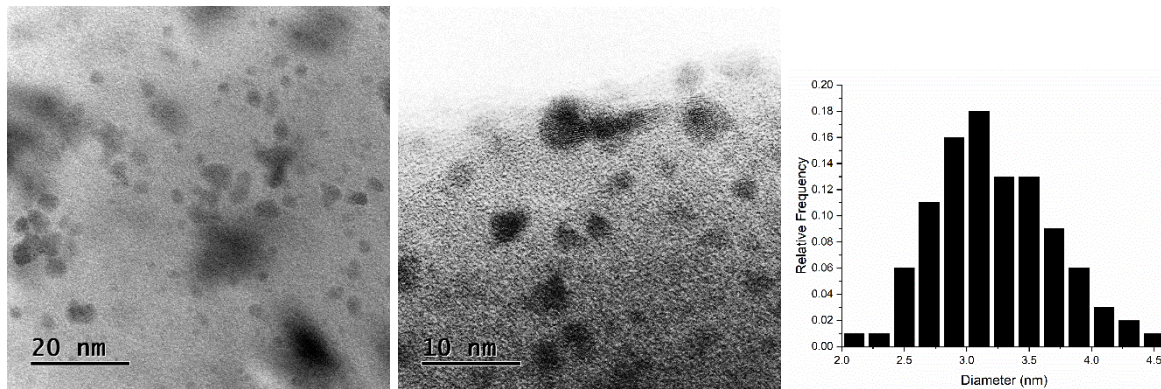


Figure S28 TEM images magnification and histogram of the **RhNPs-B** particle size distribution. Mean diameter = 3.2 ± 0.5 nm (for 100 particles)

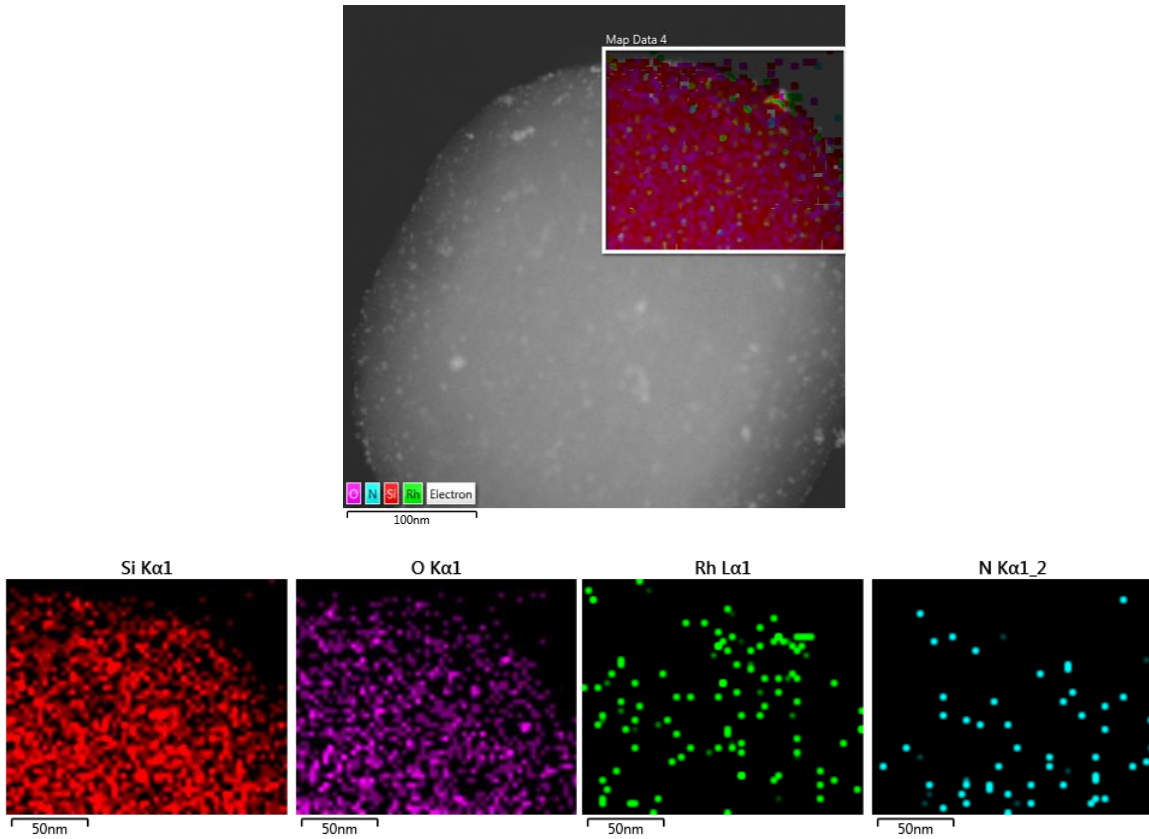


Figure S29 EDX element mapping images of **RhNPs-B**.

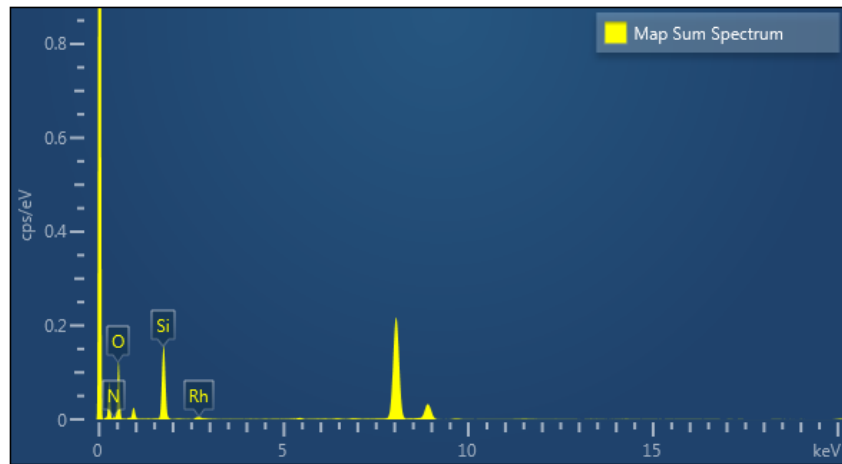


Figure S30 EDX element quantification of **RhNPs-B**.

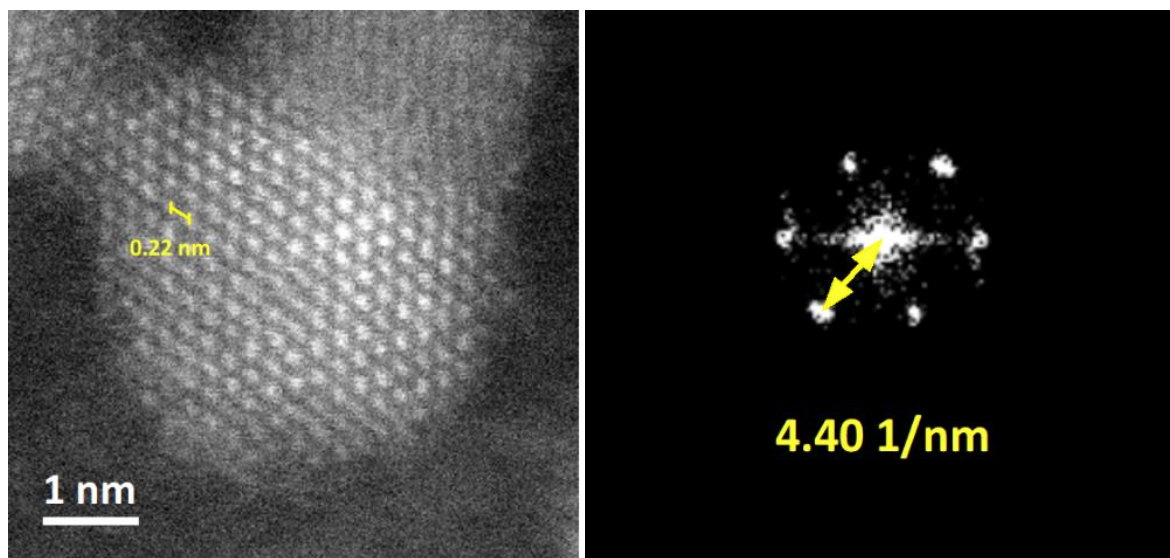


Figure S31 HR-HAADF-STEM of one Rh nanoparticle in RhNPs-B.

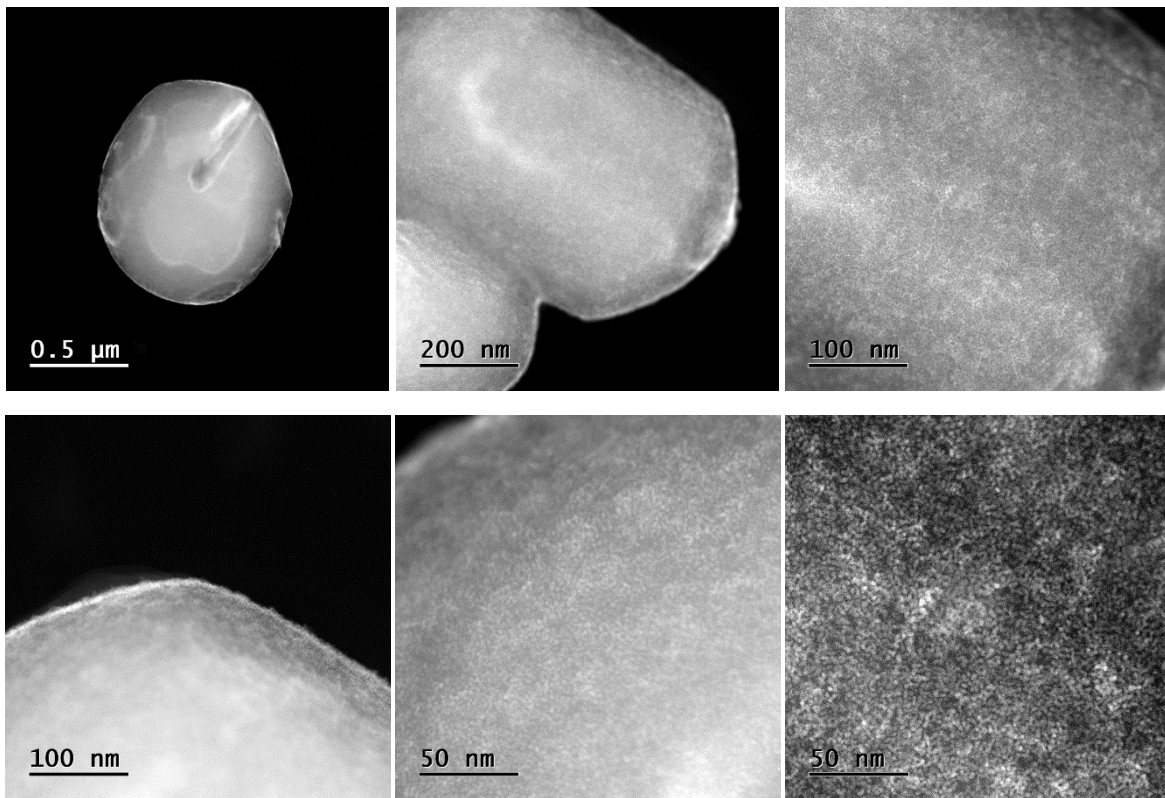


Figure S32 HAADF-STEM images of RhNPs-C

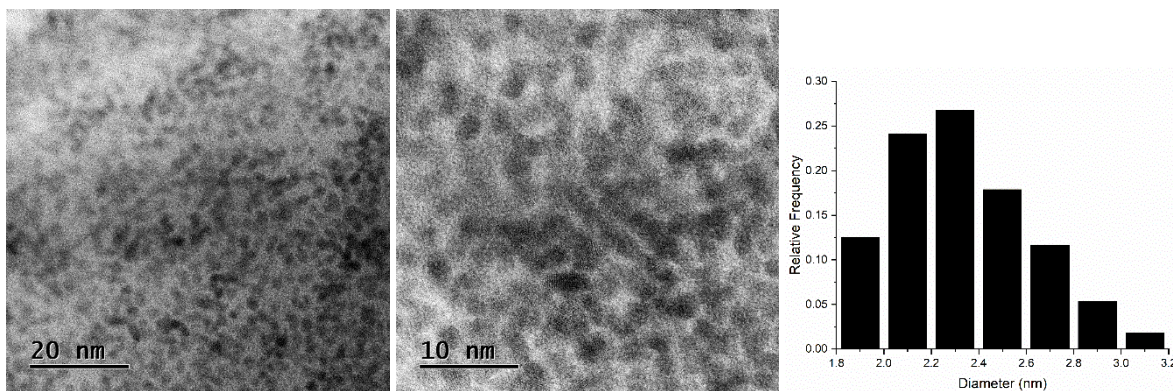


Figure S33 TEM images magnification and histogram of the RhNPs-C particle size distribution. Mean diameter = 2.3 ± 0.3 nm (for 112 particles)

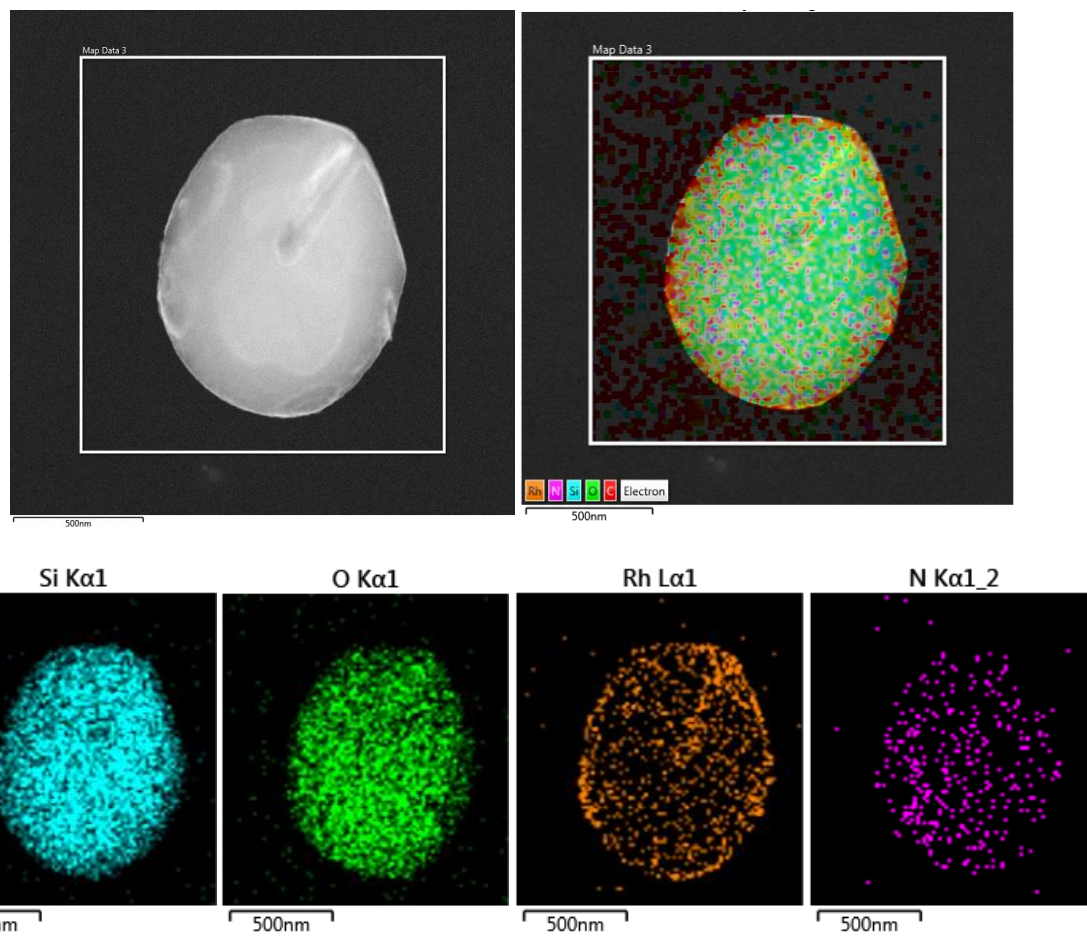


Figure S34 EDX element mapping images of **RhNPs-C**.

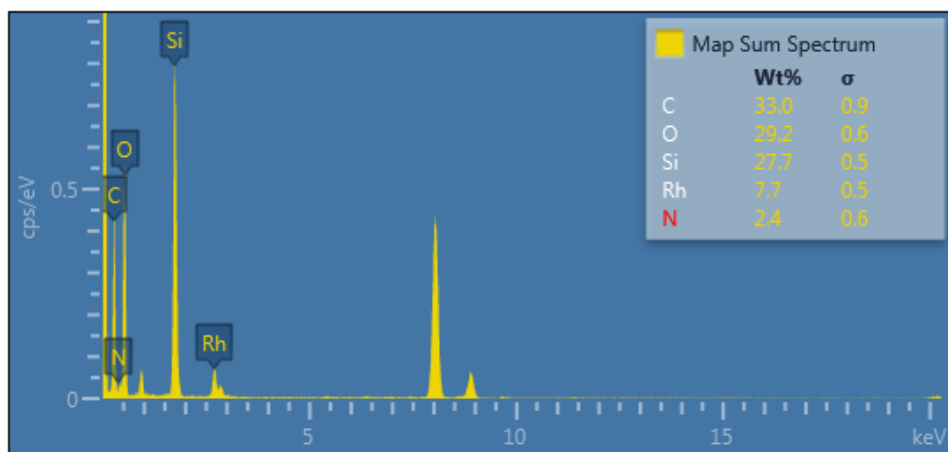


Figure S35 EDX element quantification of **RhNPs-C**.

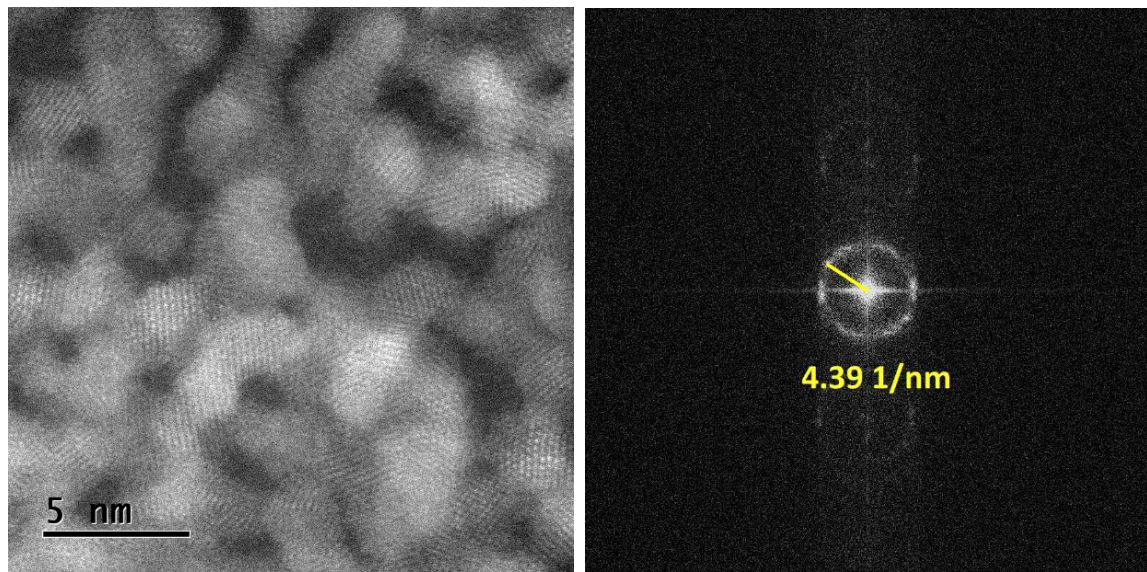


Figure S36 HR-HAADF-STEM of Rh nanoparticles in RhNPs-C.

7. BET isotherms of supported RhNPs.

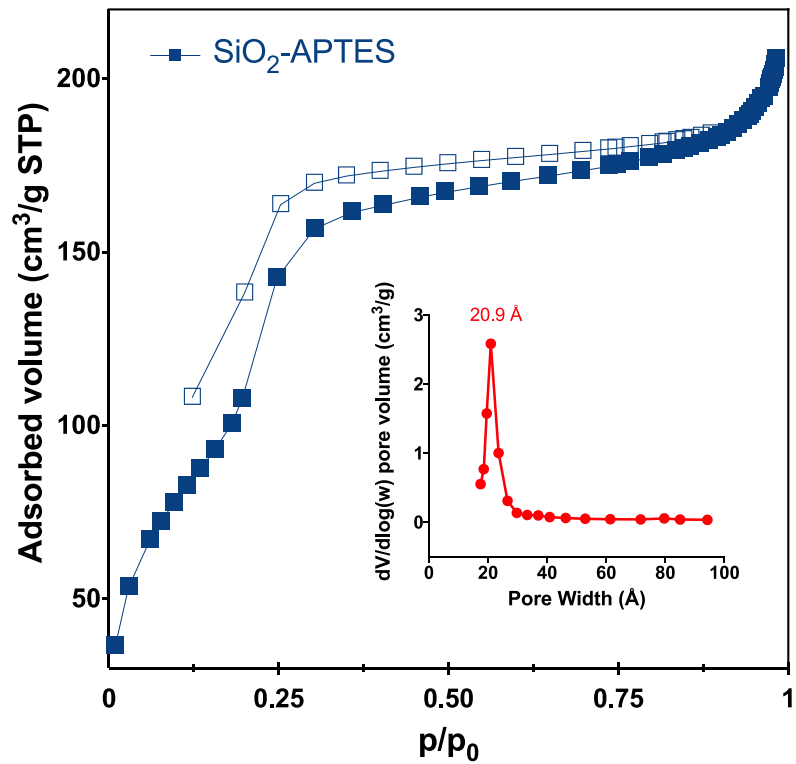


Figure S37 Adsorption-desorption isotherms of $\text{SiO}_2\text{-APTES}$ with pore size.

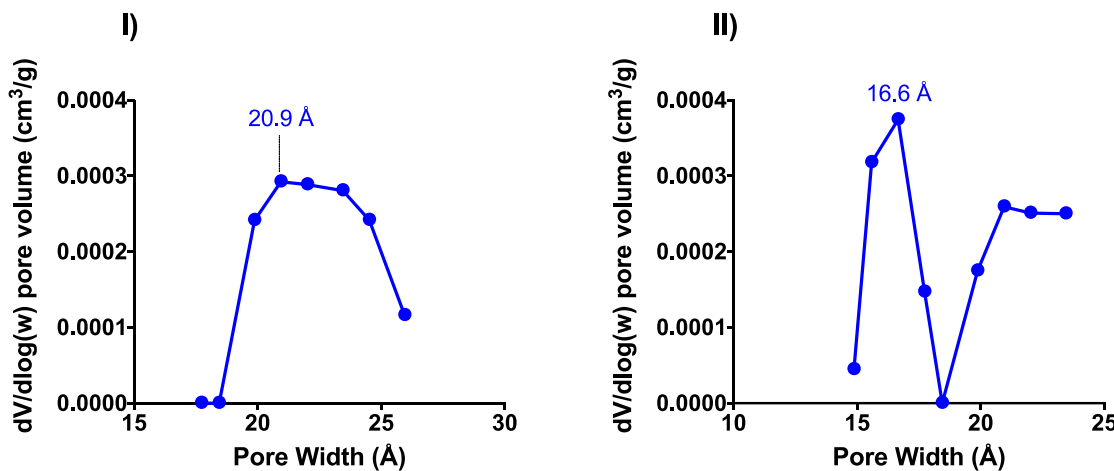


Figure S38 Pore size of I) RhNPs-B and II) RhNPs-C

Table S5 BET isotherms analysis of supported RhNPs on functionalized silicas.

Entry	Material	S_{BET} (m² g⁻¹)	Pore width (nm)
1	SiO₂-APTES	424	2.09 ^a
2	RhNPs-A	n.d.	n.d.
3	RhNPs-B	16	2.09 ^b
4	RhNPs-C	9	1.66 ^b

^a Calculated using Brunauer–Emmett–Teller (BET) model on the adsorption branch in the range of relative pressure (P/P_0) from 0.06 to 0.196..

^b Calculated using the Non-Local Density Functional Theory model (Tarazona NLDFT, Cylindrical Pores, Esf = 30.0K).

8. Selected catalytic experiments

Table S6 Substrates that are not susceptible to hydrogenation by RhNPs-B at low pressure.

Entry	Substrate	Main Product	Conversion (%) ^a	Sel. to main product (%) ^a
1	 12a	 12b	1	N.D.
2	 13	 13a	0	N.D.
3	 14	 14a	0 (0 ^b)	N.D.
4	 15	 15a	0	N.D.

Reaction conditions: 2 mmol of substrate, 5 mg of RhNPs-B (0.07 mol%), H₂ (5 bar), 2 mL of toluene, 100 °C. ^a Determined by GC using FID detector. ^b Using RhNPs-B or RhNPs-C at 40 bar of H₂ no conversion are observed.

Table S7 Optimization of reaction conditions at low pressure of the catalyzed hydrogenation of acetophenone.

Entry	Catalyst	Substrate 7 (mmol)	Time(h)	Solvent	%Conv. ^a	%Selectivity ^a			TOF (h ⁻¹) ^b
						7a	7b	7c	
1	Pristine SiO ₂	2	2	toluene	0	-	-	-	0
2	SiO ₂ -APTES	2	2	toluene	0	-	-	-	0
3	RhNPs-A	2	2	toluene	10	80	0	20	48
4	RhNPs-B	2	2	toluene	98	81	8	11	560
5	RhNPs-C	2	2	toluene	81	93	5	2	219
6	RhNPs-B	1	1	toluene	62	89	1	10	389
7	RhNPs-B	2	1	toluene	64	91	1	2	822
8	RhNPs-B	5	1	toluene	42	95	0	5	1408
9	RhNPs-B	10	1	toluene	17	94	0	6	1128
10	RhNPs-B	1	2	toluene	99	64	21	15	223
11	RhNPs-B	2	2	DMC	48	85	0	15	288
12	RhNPs-B	2	2	H ₂ O	88	94	1	5	584
13	RhNPs-B	2	2	glycerol	38	97	0	3	260
14	RhNPs-B	2	2	EtOH	84	88	7	5	521
15	RhNPs-B	2	2	heptane	64	97	2	1	438
16	RhNPs-C	2	2	heptane	>99	70	23	5	493

Reaction conditions: 2 mmol of acetophenone (7), 5 mg of catalyst [RhNPs-A (0.10 mol%); RhNPs-B (0.07 mol%); RhNPs-C (0.18 mol%)], H₂ (5 bar), 100 °C. ^aDetermined by GC using FID detector. ^b TOF= mmol of principal product x (mmol of Rh x h)⁻¹

Table S8 RhNPs-B catalyst reuse in the hydrogenation of cyclohexene in toluene.

Run	Conversion (%) ^a	TOF (h ⁻¹) ^c	Hydrogenation of cyclohexene (2) to 2a	
			2	2a
1	99	705		
2	99	705		
3	99	705		
4	99	705		
5	99	705		

Reaction conditions: 2 mmol of cyclohexene (2), 5 mg of RhNPs-B (0.07 mol%), 2 mL of toluene, H₂ (5 bar), 100 °C, 2h. ^aDetermined by GC using FID detector. ^bAt the end of each reaction all volatiles are evaporated and collected for GC analysis then new acetophenone and toluene are added. ^c TOF= mmol of principal product x (mmol of Rh x h)⁻¹

Table S9 RhNPs-C catalyst reuse in the hydrogenation of cyclohexene in heptane.

Run ^b	Conversion (%) ^a	TOF (h ⁻¹) ^c
1	99	270
2	99	270
3	99	270
4	99	270
5	99	270

Reaction conditions: 2 mmol of cyclohexene (2), 5 mg of **RhNPs-C** (0.07 mol%), 2 mL of **heptane**, H₂ (5 bar), 100 °C, 2h. ^a Determined by GC using FID detector. ^b At the end of each reaction all volatiles are evaporated and collected for GC analysis then new acetophenone and heptane are added. ^c TOF= mmol of principal product x (mmol of Rh x h)⁻¹

9. TEM images and EDX analysis after use in the catalyzed acetophenone hydrogenation

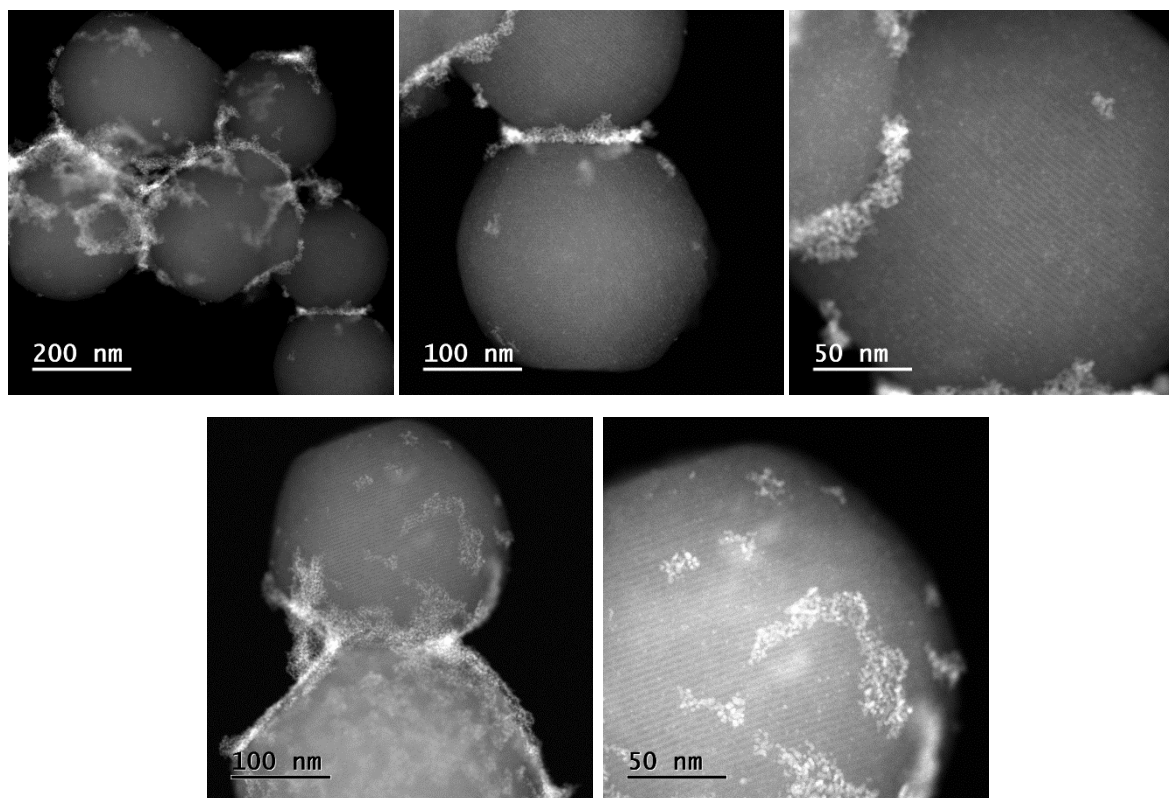


Figure S39 HAADF-STEM images of **RhNPs-B** after acetophenone hydrogenation (40 bar).

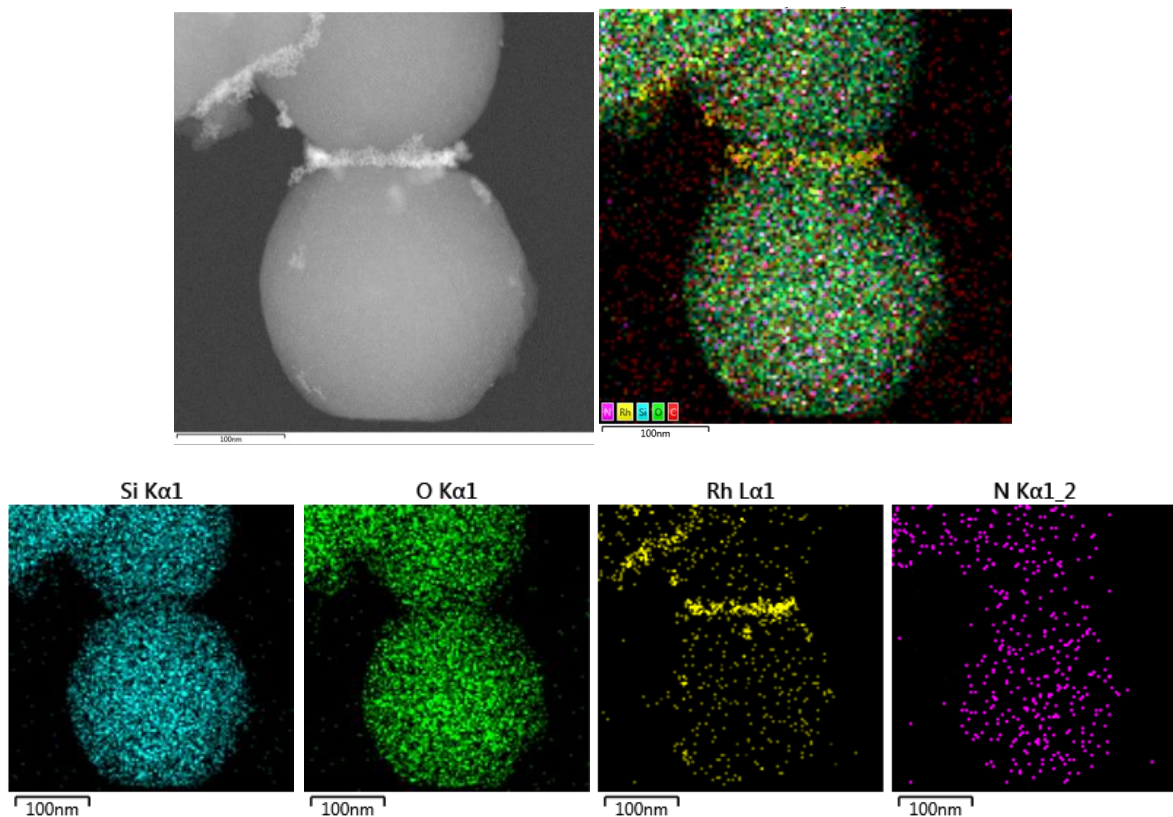


Figure S40 EDX element mapping images of **RhNPs-B** after acetophenone hydrogenation (40 bar).

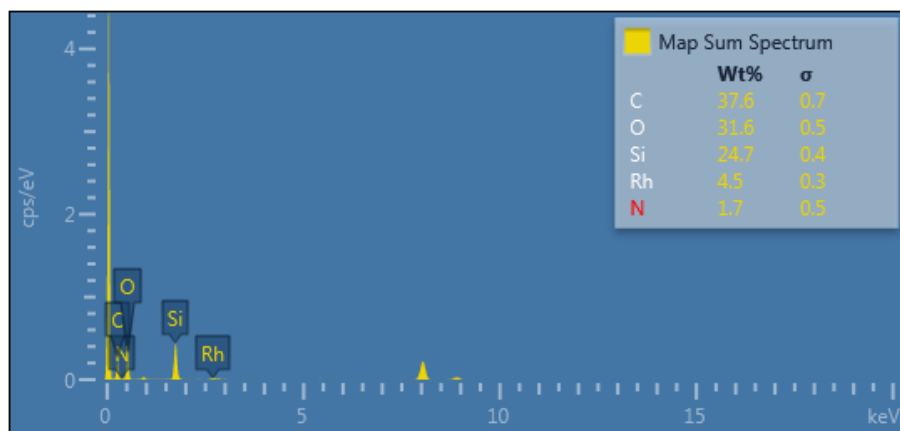


Figure S41 EDX element quantification of **RhNPs-B** after acetophenone hydrogenation (40 bar).

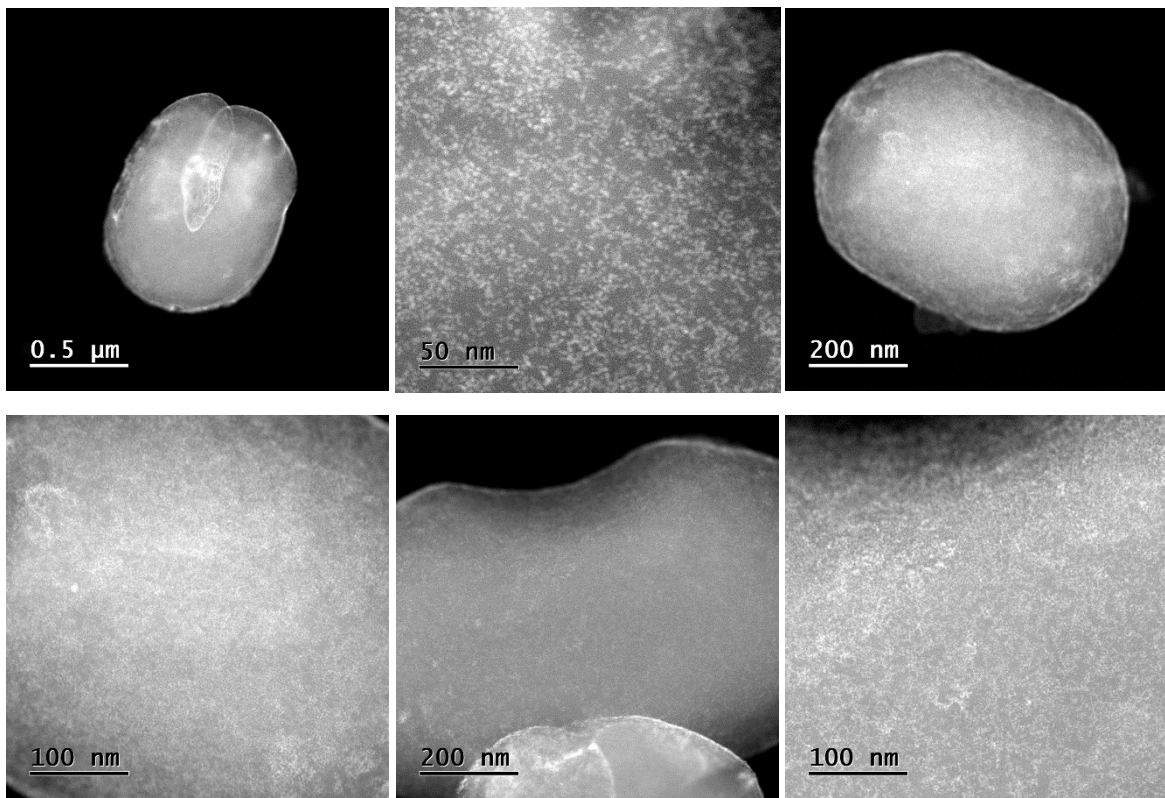


Figure S42 HAADF-STEM images of **RhNPs-C** after acetophenone hydrogenation (40 bar).

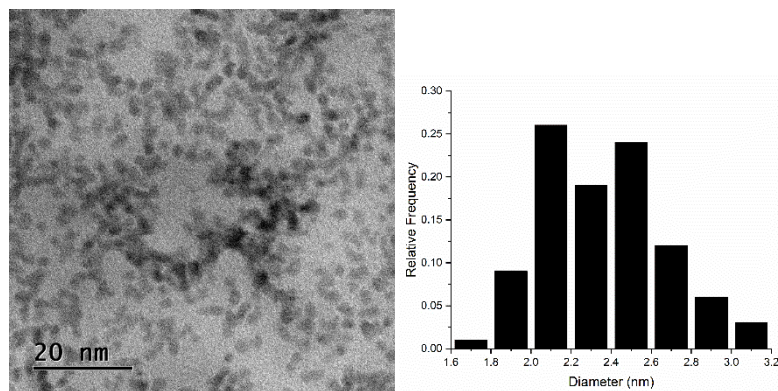


Figure S43 TEM image magnification and histogram of the **RhNPs-C** particle size distribution after acetophenone hydrogenation (40 bar). Mean diameter = 2.3 ± 0.3 nm (for 100 particles)

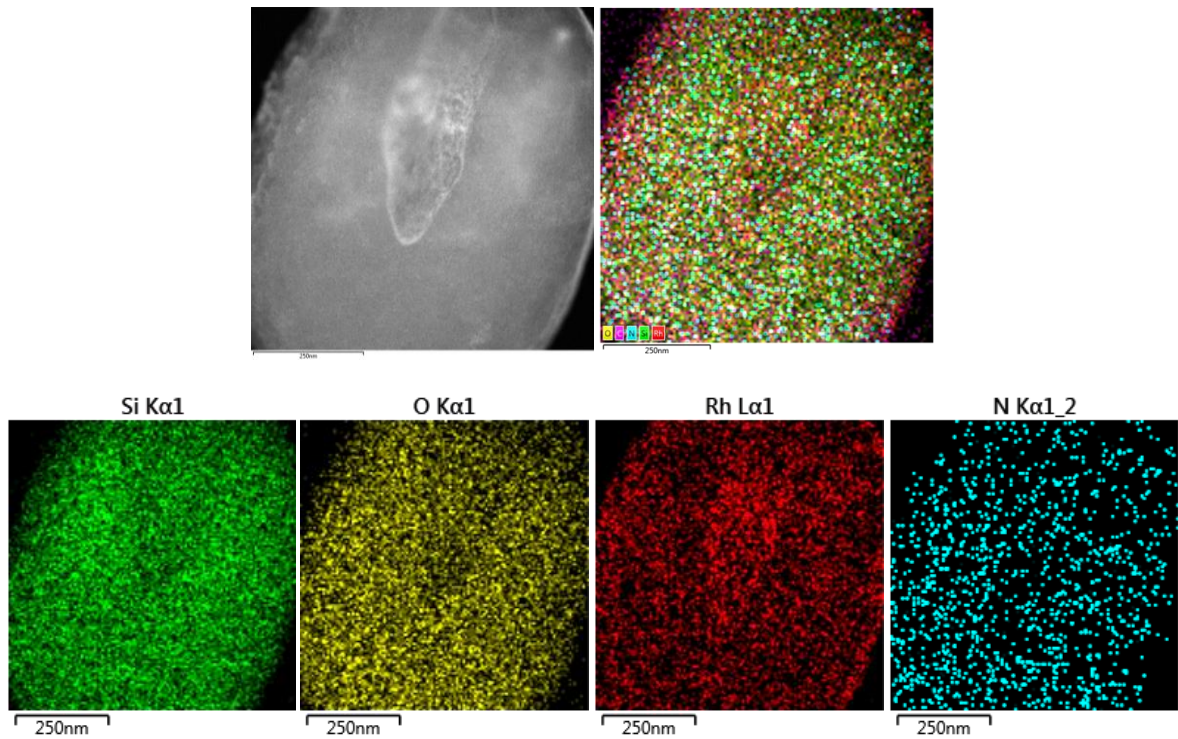


Figure S44 EDX element mapping images of RhNPs-C after acetophenone hydrogenation (40 bar).

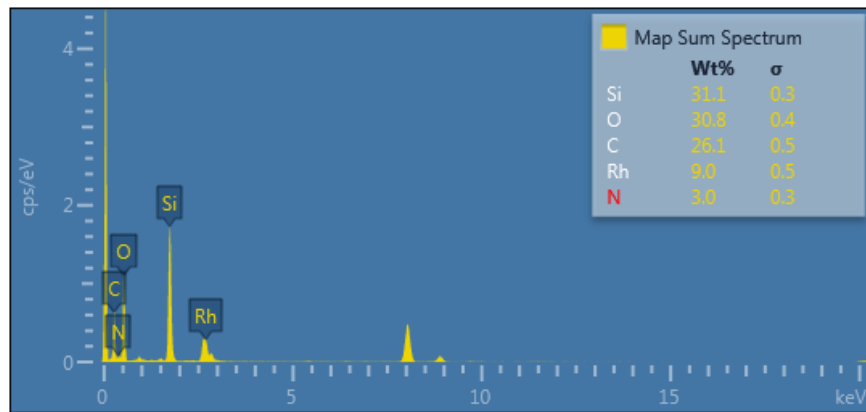


Figure S45 EDX element quantification of RhNPs-C after acetophenone hydrogenation (40 bar).